Neotropical Ichthyology

Original article

https://doi.org/10.1590/1982-0224-2025-0156

urn:lsid:zoobank.org:pub:DA5A875F-CDB7-4633-B432-E7902154C8AB

Morphological and molecular evidence reveals two new species of *Cambeva* (Siluriformes: Trichomycteridae) from the rio Paraná basin, Paraná State, Brazil

Isadora Carolina Martins[1], Renan B. dos Reis[1,2,3], Bruno Henrique Mioto Stabile[2], Alessandra Valéria de Oliveira[1,2,4] and Weferson Júnio da Graça[1,2,4,5]

Correspondence:
Isadora Carolina Martins
icmartins@outlook.com.br

The rio Paraná basin represents a highly dynamic hydrographic system shaped by geological events that promoted the dispersal and diversification of its ichthyofauna, including trichomycterid species of *Cambeva*. Recent field surveys in tributaries of the upper and lower rio Paraná ecoregions, in the state of Paraná, revealed two previously undescribed species. In this context, the present study aims to describe them based on morphological evidence, including diagnostic characters related to color pattern and meristic data, as well as molecular evidence derived from DNA barcoding using the mitochondrial COI gene. Phylogenetic analyses under Maximum Likelihood and Bayesian Inference recovered both species as sister lineages, forming a clade with *C. perobana*. Species delimitation analyses (ASAP, PTP, and mGMYC) supported their recognition as independent evolutionary lineages, whereas the sGMYC analysis showed incongruence. Genetic distances between the new species were 2% (K2P), and both exhibited divergences greater than 2% from the congeners included in the analysis. The new species exhibit distinct distribution patterns, possibly associated with environmental heterogeneity and the complexity of the rio Paraná basin drainage network.

Keywords: Cytochrome c oxidase subunit I (COI), Genetic diversity, Ichthyofauna, Species identification, Trichomycterinae.

Submitted December 3, 2025
Accepted September 9, 2026
Epub ???, 2026

Associate Editor George Mattox
Section Editor William Crampton
Editor-in-chief José Birindelli

1 Universidade Estadual de Maringá, Centro de Ciências Biológicas, Departamento de Biologia, Coleção Ictiológica do Nupélia, Av. Colombo, 5790, 87020-900, Maringá, PR, Brazil. (ICM) icmartins@outlook.com.br (corresponding author), (RBR) reis.renanb@gmail.com, (AVO) avoliveira@uem.br, (WJG) weferson@nupelia.uem.br.

2 Universidade Estadual de Maringá, Centro de Ciências Biológicas, Departamento de Biotecnologia, Genética e Biologia Celular, Programa de Pós-Graduação em Ecologia de Ambientes Aquáticos Continentais, Maringá, PR, Brazil. (BHMS) bhmstabile@gmail.com.

3 Universidade Estadual do Oeste do Paraná, Centro de Ciências Biológicas e da Saúde, Programa de Pós-Graduação em Conservação e Manejo de Recursos Naturais, Rua Universitária, 2069, 85819-110, Cascavel, PR, Brazil.

4 Universidade Estadual de Maringá, Centro de Ciências Biológicas, Instituto de Pesquisas em Limnologia, Ictiologia e Aquicultura, Maringá, PR, Brazil.

5 Universidade Estadual de Maringá, Centro de Ciências Biológicas, Programa de Pós-Graduação em Biologia Comparada, Maringá, PR, Brazil.

Online version ISSN 1982-0224
Print version ISSN 1679-6225

Neotrop. Ichthyol.
vol. 24, no. 4, 2026

A bacia do rio Paraná representa um sistema hidrográfico altamente dinâmico, moldado por eventos geológicos que propiciaram a dispersão e diversificação de sua ictiofauna, incluindo espécies de trichomicterídeos pertencentes a *Cambeva*. Levantamentos de campo recentes em afluentes das ecorregiões do alto e baixo rio Paraná, no estado do Paraná, revelaram duas espécies ainda não descritas. Nesse contexto, este trabalho objetiva descrevê-las com base em evidências morfológicas, incluindo caracteres diagnósticos relacionados ao padrão de coloração e a dados merísticos, e evidências moleculares resultantes de DNA-barcode, utilizando o marcador mitocondrial do gene COI. Análises filogenéticas por Máxima Verossimilhança e Inferência Bayesiana recuperaram ambas as espécies como linhagens irmãs, formando um clado com *C. perobana*. As análises de delimitação de espécies (ASAP, PTP e mGMYC) corroboraram seu reconhecimento como linhagens evolutivas independentes, enquanto a análise de sGMYC mostrou incongruência. A distância genética entre as novas espécies foi de 2% (K2P), e ambas apresentaram distâncias superiores a 2% em relação às congêneres utilizadas na análise. As novas espécies apresentam distribuições distintas, possivelmente associadas à heterogeneidade ambiental e à complexidade da rede de drenagem da bacia do rio Paraná.

Palavras-chave: Citocromo c oxidase subunidade I (COI), Diversidade Genética, Ictiofauna, Identificação de espécies, Trichomycterinae.

INTRODUCTION

The rio Paraná basin is the second largest drainage system in South America (Stevaux, 1994; Agostinho *et al*., 1995), extending across Brazil, Paraguay, and Argentina (Agostinho *et al*., 2007). Beyond its large geographic extent, the basin represents a highly dynamic hydrographic system shaped by geological and climatic events that promoted drainage rearrangements, headwater captures, and connections among adjacent ecoregions (dos Reis *et al*., 2025a). These processes have facilitated dispersion and secondary contact among freshwater lineages, while also promoting isolation in tributary sub-basins, creating favorable conditions for diversification (Hubert, Renno, 2006; Cassemiro *et al*., 2023; dos Reis *et al*., 2025a). In the state of Paraná, this basin is divided into the upper and lower rio Paraná ecoregions (Abell *et al*., 2008), separated by the Sete Quedas Falls, a biogeographic barrier now submerged by the Itaipu Reservoir (Agostinho *et al*., 1995). The upper rio Paraná includes several sub-basins (Bonetto *et al*., 1986; Britski, Langeani, 1988; Dagosta *et al*., 2024), such as the rio Piquiri basin (Maack, 1981; Morais-Silva *et al*., 2018), whereas the lower rio Paraná comprises tributaries downstream of the former Sete Quedas Falls, including the rios São Francisco Verdadeiro, São Francisco Falso, and Guaçu (Paraná, 2013). The interplay between historical barriers and more recent dispersion routes has likely contributed to the high diversity and complex phylogeographic patterns observed in freshwater fishes of the basin, including trichomycterids.

Trichomycteridae is one of the most diverse families of Siluriformes, with 495 valid species (Fricke *et al*., 2026a), distributed throughout South America and Central America (de Pinna, Wosiacki, 2003). Within the family, Trichomycterinae is the richest subfamily with 361 valid species (Fricke *et al*., 2026a). Among its genera, *Cambeva* Katz, Barbosa, Mattos & Costa, 2018, comprises species distributed in the Paraná, São Francisco, Ribeira de Iguape, and Uruguay rivers basin, including portions of these drainages in Argentina and Uruguay, as well as in small coastal basins of southeastern and southern Brazil (Katz *et al*., 2018). Currently, 72 valid species of *Cambeva* are known (Fricke *et al*., 2026b), and recent phylogenetic and taxonomic studies have highlighted the complexity of species limits within the genus. In the upper rio Paraná basin in the state of Paraná, four species of *Cambeva* have been recorded: *C. davisi* (Haseman, 1911), *C. diabola* (Bockmann, Casatti & de Pinna, 2004), *C. horacioi* dos Reis, Frota, Fabrin & Graça, 2019, and *C. perobana* Martins, dos Reis, Stabile & da Graça, 2024. Of these, two (*C.* aff. *davisi* and *C. perobana*) occur in the rio Piquiri basin (dos Reis *et al*., 2020a; Martins *et al*., 2024). In contrast, only *C.* aff. *davisi* was identified for the lower rio Paraná basin in the state of Paraná (Pereira *et al*., 2021). However, recent fish collections in both the upper and lower rio Paraná basins revealed species that do not conform to the diagnoses of any currently described species, indicating that the diversity of *Cambeva* in the Paraná River basin may be underestimated.

Species of *Cambeva* are known to exhibit considerable variation in color pattern (Donin *et al*., 2022; Martins *et al*., 2024; dos Reis *et al*., 2025a), which may complicate species identification based solely on external morphology (Silva *et al*., 2010; Nascimento *et al*., 2017; Donin *et al*., 2022). Although recent taxonomic efforts have expanded the knowledge of the genus, species boundaries in several lineages remain difficult to define (Donin *et al*., 2022). Therefore, species delimitation requires consideration of aspects such as ontogeny, geographical variations and habitat specificity, beyond external morphology (see Arratia *et al*., 1978; Silva *et al*., 2010; Ferrer, Malabarba, 2013; Nascimento *et al*., 2017; Donin *et al*., 2020). In this context, molecular analyses using the cytochrome c oxidase subunit I (COI) gene have proven to be an important tool for species delimitation (Hebert *et al*., 2003; Hanner *et al*., 2011), particularly in groups with complex taxonomy such as *Cambeva*.

Thus, based on morphological and molecular evidence, this study describes two new species of *Cambeva* from the rio Piquiri basin (upper rio Paraná) and tributaries of the left bank of the lower rio Paraná, contributing to a better understanding of the genus diversity and distribution in these ecoregion.

MATERIAL AND METHODS

Collection data and study area. The samples were collected at different locations in the basins of the rio Piquiri (upper rio Paraná) and in tributaries of the lower rio Paraná basin, including the rios São Francisco Falso, São Francisco Verdadeiro, and Arroio Guaçu, in the state of Paraná, Brazil.

Specimens were anesthetized and euthanized with benzocaine, according to Resolution 1000/2012 proposed by the Federal Council of Veterinary Medicine, Brazil. They were then fixed in 10% formalin for morphological analysis or in 99% ethanol for molecular studies and housed at Coleção Ictiológica do Nupélia (NUP).

Morphological data. The morphometric data of the specimens were obtained point by point with a digital caliper (precision of 0.1 mm) on the left lateral view, following Tchernavin (1944), Costa (1992), Nascimento *et al*. (2017), and Donin *et al*. (2022), according to adaptations and descriptions of the measurements made by Martins *et al*. (2024). Morphological comparisons were based on external morphology, color pattern, morphometry, meristic counts and osteological characters. The color pattern was standardized following the nomenclature of the types of spots, blotches, and stripes of dos Reis *et al.* (2025a). Non-type specimens are poorly preserved specimens. Comparisons were made with examined specimens of congeneric species (see comparative material), comparative material analyzed by dos Reis *et al*. (2023, 2025b), and with original descriptions of additional taxa such as *Cambeva atrobrunnea* Costa, Feltrin & Katz, 2024, *C. galactica* Costa, Feltrin & Katz, 2024, *C. luteoreticulata* Costa, Feltrin & Katz, 2024, *C. rotundipinna* Costa, Feltrin & Katz, 2024 (Costa *et al*., 2024).

Osteological analyses were carried out using the clearing and staining method of Taylor, Van Dyke (1985) on five specimens of the first new species described herein and two of the second. All osteological counts and observations refer exclusively to cleared and stained (c&s) specimens. Vertebral counts exclude the vertebrae of the Weberian complex, and the compound caudal centrum (PU1+U1) was counted as a single element. The nomenclature of bones and cartilages, laterosensory canals, and associated pores follows Bockmann *et al.* (2004). Counts of unbranched rays and branched rays are represented in uppercase Roman numerals and Arabic numerals, respectively, following Bockmann *et al*. (2004). The asterisk indicates counts made on the holotype, and each meristic characteristic has the number of specimens analyzed in brackets. The abbreviation SL refers to standard length. Osteological illustrations were based on photographs taken under a stereomicroscope and on direct observation of the cleared and stained (c&s) specimens.

Molecular data. DNA was extracted from the muscle tissue of the specimens using the Wizard® Genomics DNA Purification kit (Promega®), following the manufacturer's instructions. The concentration of DNA present in each sample was estimated using a NanoDrop™ Lite spectrophotometer (Thermo Fisher Scientific®). Amplification took place from the partial fragment of the subunit I gene of the mitochondrial protein cytochrome c oxidase (COI), using the primers FishF1 5'-TCAACCAACCACAAAGACATTGGCAC-3' (Ward *et al*., 2005) and FR1d 5'-CACCTCAGGGTGTCCGAARAAYARAA-3' (Ivanova *et al*., 2007). The polymerase chain reaction (PCR) was carried out in 25 µL of suspension containing Tris-KCl reaction buffer (20 mM Tris-HCl pH 8.4, 50 mM KCl), $MgCl^2$ (1.5 mM), primers (2.5 µM each), dNTP (0.1 mM each), 1 U Platinum™ Taq DNA polymerase (5 U/µL, Invitrogen) and 10 ng of template DNA. The PCR conditions consisted of an initial denaturation cycle of 2 min (94°C), followed by 35 cycles of 30 sec of

denaturation (94°C), 1 min and 30 sec of annealing (50°C), 1 min and 30 sec of extension (72°C) and a final extension of 10 min (72°C). After amplification, the PCR products were analyzed on a 1% agarose gel, and the size of the fragments obtained was estimated using the standard 100 bp DNA Ladder marker. Purification of the PCR products followed the procedures described in Rosenthal *et al*. (1993). Sequencing was carried out using an ABI 3500 Applied Biosystems® automated sequencer.

The electropherograms obtained from the sequencing were edited manually using the BioEdit program (Hall, 1999) and MEGA 11 (Tamura *et al*., 2021). After editing, the sequences were also aligned in MEGA 11 with ClustalW (Thompson *et al*., 1994), and the genetic distances between all the sequences and between the species groups were calculated using the Kimura-2-Parameter (K2P) model. Also in MEGA 11, the best-fit nucleotide substitution model was determined based on the Bayesian Information Criterion (BIC), selecting the TN93+G model (lowest BIC score: 6096.049, with 185 parameters). A maximum likelihood (ML) analysis was then performed using this model, with 1,000 bootstrap replicates. The haplotypes were characterized and haplotypic diversity was calculated using DnaSP v. 6 (Rozas *et al*., 2017).

The Bayesian tree was created using an uncorrelated relaxed molecular clock and a coalescent tree prior (Constant Size), on an arbitrary time scale, using BEAST v. 1.8.4 (Drummond *et al*., 2012). A random tree was used as the initial tree for the MCMC searches, with a run of 50 million generations, and a tree sampled every 5,000 generations. Tracer v. 1.7.2 (Rambaut *et al*., 2018) was used to determine the stationary phase and an effective sample size, *i.e*., ESS value > 200 for the parameters analyzed. Ten percent of the chain was discarded as a burn-in procedure, and the remaining trees were used to find the Maximum Clade Credibility Tree (MCC) (Drummond *et al*., 2012) in TreeAnnotator v. 1.8.4 (included in BEAST). The resulting ultrametric tree was visualized in FigTree v. 1.4.3 (Rambaut, 2019).

Sequences of different *Cambeva* species previously deposited in GenBank were used (Tab. **S1**), in addition to the sequence of *Trichomycterus nigricans* Valenciennes, 1832 (MN385796), which was used as the outgroup when constructing the phylogenetic tree. Although *Scleronema* Eigenmann, 1917 is recognized as the sister group of *Cambeva*, *T. nigricans* was used as the outgroup because the available COI sequence presented greater length and higher overlap with our dataset, minimizing missing data and improving alignment quality. The new sequences obtained were deposited in GenBank under the access codes PV560700 and PV560701 for specimens collected in São Pedro do Iguaçu (rio São Francisco Falso basin), PV560705 and PV560706 for specimens collected in Toledo (rio São Francisco Verdadeiro basin), and PV915783 for the specimen collected in Cascavel (rio Piquiri basin). Access to the species genetic heritage was authorized by the National System for the Management of Genetic Heritage and Associated Traditional Knowledge (SisGen), under registration number A37B37F.

Delimitation methods. Three different molecular species delimitation methods were employed as part of an iterative taxonomic framework for testing species boundaries: Assemble Species by Automatic Partitioning (ASAP; Puillandre *et al*., 2021), Poisson Tree Process (PTP; Zhang *et al*., 2013), and General Mixed Yule Coalescent Approach (GMYC; Pons *et al*., 2006; Fujisawa, Barraclough, 2013). These methods were selected because they rely on different analytical frameworks, including

distance-based and tree-based approaches, providing complementary perspectives on species boundaries alongside morphological evidence.

The first method was performed using iTaxoTools (Vences *et al*., 2021) software, using ASAP implementation and the fasta alignment file. This analysis was performed using the complete dataset of 163 sequences, as ASAP relies exclusively on genetic distance matrices and does not impose restrictions on the inclusion of identical haplotypes. It automatically detects partitions that maximize separation between groups by identifying barcode gaps for different lineages (Puillandre *et al*., 2021).

For the PTP method, the maximum likelihood tree was used as input on the PTP web server (https://species.h-its.org/) with default parameters. The complete dataset was used, as PTP does not require the reduction to unique haplotypes. The PTP method is based on modeling the number of substitutions along the branches of a non-ultrametric phylogenetic tree, thus short branches are interpreted as a result of coalescent processes within species, while longer branches reflect speciation events (Zhang *et al*., 2013).

For the GMYC method, the same Bayesian tree described in the phylogenetic analyses section was used as input. This tree was inferred from single haplotypes, which is a technical requirement of the GMYC method, as the construction of the ultrametric tree does not allow sequences with zero-length branches, arising from identical haplotypes. A Newick-format tree was used as the input file for this analysis and was entered into the web server (https://specifications.org/gmyc/). The method employs a single-locus molecular delimitation approach using an ultrametric tree to identify independently evolving lineages (Fujisawa, Barraclough, 2013). Two evolutionary models are combined: a model of interspecific diversification under a Yule process and a coalescent model to describe intraspecific relationships (Fujisawa, Barraclough, 2013). The transition point(s) in the ultrametric tree that separate species-level processes from population-level processes are estimated under a maximum-likelihood framework (Fujisawa, Barraclough, 2013).

In this study, two approaches were applied: single-threshold (sGMYC), in which a single point in time separates all species diversification events from coalescence events, and multiple threshold (mGMYC), in which it relaxes the premise of the single version that speciation events are older than all coalescence events in the gene tree (Fujisawa, Barraclough, 2013). All species contained in the Bayesian tree were used in the species delimitation analysis; however, a crop of the tree was made to demonstrate only the results for the two new species in the genus and the outgroup. The results of the delimitation of congeneric species are presented as supplementary material.

Geographic distribution analyses. The map was created using QGIS software v. 3.32.3 and assembled from data (shapefiles) from the Brazilian Institute of Geography and Statistics (IBGE; https://www.ibge.gov.br/geociencias/organizacao-do-territorio/malhas-territoriais/15774-malhas.html) and the National Water and Sanitation Agency (ANA; https://www.iat.pr.gov.br/Pagina/Mapas-e-Dados-Espaciais). The conservation status follows the guidelines of the International Union for Conservation of Nature for the Red List of Threatened Species (IUCN, 2024). The extent of occurrence (EOO) and area of occupation (AOO) were calculated using the GeoCat web server (http://geocat.kew.org/).

RESULTS

Taxonomic accounts

Cambeva marginimaculata, new species

urn:lsid:zoobank.org:act:8D4A41AD-64FE-4E2C-B011-4FA5D0699135

(Figs. 1–8; Tab. 1)

Trichomycterus sp. —Pereira *et al*., 2014:4 (Ichthyofauna of urban streams in the western region of Paraná State, Brazil; *partim*: NUP 14591).

Holotype. NUP 25055, 43.1 mm SL, Brazil, Paraná State, municipality of Cascavel, unnamed stream, tributary of rio Melissa, rio Piquiri basin, upper rio Paraná, 24°56'12"S 53°24'26"W, 1 Nov 2023, R. B. dos Reis, B. H. M. Stabile, M. Z. Rollof & C. E. V. Grou.

Paratypes. All from Brazil, Paraná State. Upper rio Paraná basin: rio Piquiri basin: MZUEL 24223, 1, 47.8 mm SL, municipality of Palotina, rio Santa Fé, tributary of rio São Camilo, 24°20'47"S 53°51'00"W, 29 Jul 2013, A. M. Cunico. NUP 16690, 5, 25.3–42.6 mm SL, municipality of Palotina, rio Pioneiro, 24°22'11"S 53°49'34"W, 5 May 2014, A. M. Cunico. NUP 16695, 2, 50.2–55.3 mm SL, municipality of Palotina, rio Pioneiro, tributary of rio Piquiri, 24°22'11"S 53°49'34"W, 5 May 2014, A. M. Cunico. NUP 16736, 1, 36.6 mm SL, municipality of Palotina, rio São Camilo, tributary of rio Piquiri, 24°11'40"S 53°54'02"W, 5 May 2014, A. M. Cunico. NUP 18047, 27, 21.5–70.4 mm SL, municipality of Palotina, riacho Quati, tributary of rio São Camilo, 24°18'29"S 53°54'24"W, 15 Oct 2015, A. L. Pereira & A. J. Francelina. NUP 21195, 4, 48.0–97.0 mm SL, municipality of Cascavel, rio Piquirizinho, tributary of rio Piquiri, 25°04'13"S 53°11'23"W, 1 Feb 2018, R. L. Delariva & C. Larentis. NUP 22435, 8, 30.0–73.0 mm SL, municipality of Brasilândia do Sul, rio das Antas, 24°12'19"S 53°28'00"W, 7 May 2019, A. M. Cunico. NUP 22458, 1, 66.0 mm SL, municipality of Terra Roxa, córrego Taquari, 24°07'35"S 54°02'49"W, 7 Feb 2019, A. M. Cunico. NUP 22499, 14, 22.0–62.0 mm SL, municipality of Francisco Alves, rio do Bagre, 24°06'40"S 53°51'56"W, 29 Mar 2018, A. M. Cunico. NUP 22572, 3, 46.0–69.0 mm SL, municipality of Palotina, rio Santa Fé, 24°17'36"S 53°51'12"W, 7 Feb 2019, A. M. Cunico. NUP 24849, 4, 40.9–53.4 mm SL, municipality of Cascavel, unnamed stream, tributary of rio Melissa, 24°56'12"S 53°24'26"W, 1 Nov 2023, R. B. dos Reis, B. H. M. Stabile, M. Z. Rollof & C. E. V. Grou. NUP 25879, 1 c&s, 40,7 mm SL, municipality of Cascavel, unnamed stream, tributary of rio Melissa, 24°56'12"S 53°24'26"W, 1 Nov 2023, R. B. dos Reis, B. H. M. Stabile, M. Z. Rollof & C. E. V. Grou. NUP 25902, 3, 34.5–49.0 mm SL, municipality of Cascavel, unnamed stream, tributary of rio Melissa, 24°56'12"S 53°24'26"W, 1 Nov 2023, R. B. dos Reis, B. H. M. Stabile, M. Z. Rollof & C. E. V. Grou. Lower rio Paraná basin: arroio Guaçu: NUP 3046, 11, 17.7–61.5 mm SL, municipality of Marechal Cândido Rondon, Ribeirão Lageado, rio Guaçu, 24°32'S 54°01'W, 23 Jan 2005, G. Baumgartner. Rio São Francisco Verdadeiro: MHNCI

13134, 9, 19.5–42.4 mm SL, municipality of Cascavel, córrego São Francisco, tributary of rio das Antas, 24°56'19"S 53°28'16"W, 1 Jun 2010, Gerpel. NUP 4711, 5, 35.7–64.3 mm SL, municipality of Toledo, rio do Cedro, 24°44'43"S 53°46'09"W, 21 Apr 2006, Gerpel. NUP 8558, 2, 64.0–96.0 mm SL, municipality of Toledo, rio Pinheirinho, tributary of rio Toledo, 24°45'23"S 53°42'33"W, 11 Jun 2008, Gerpel. NUP 8559, 4, 22.0–49.0 mm SL, municipality of Toledo, rio Pinheirinho, tributary of rio Toledo, 24°45'23"S 53°42'33"W, 11 Jun 2008, Gerpel. NUP 14591, 92, 32.0–69.3 mm SL, municipality of Toledo, córrego Pinheirinho, tributary of rio Toledo, 24°44'46"S 53°42'48"W, 1 Jun 2010, Gerpel. NUP 25877, 4 c&s, 42.3–60.8 mm SL, municipality of Toledo, córrego Pinheirinho, tributary of rio Toledo, 24°44'46"S 53°42'48"W, 1 Jun 2010, Gerpel. UFRGS 30244, 20, 27.0–63.0 mm SL, municipality of Toledo, rio Pinheirinho, 24°45'23"S 53°42'33"W, 20 Feb 2008, Gerpel.

Diagnosis. *Cambeva marginimaculata* differs from all congeners, except *C. panthera* Costa, Feltrin & Katz, 2021 and *C. gamabelardense* Costa, Feltrin & Katz, 2022, by the presence of rounded brown blotches of variable size, irregular shape with darker brown margins sometimes connected forming ring-like blotches, and never forming continuous stripes (Figs. 1–2) (*vs.* uniformly pigmented spots or blotches without darker margins, or absence of spots, blotches or stripes; or presence of continuous stripes on the lateral surface of the body). *Cambeva marginimaculata* differs from your



FIGURE 1 | *Cambeva marginimaculata*, NUP 25055, holotype, 43.1 mm SL, unnamed stream, tributary of rio Melissa, rio Piquiri basin, municipality of Cascavel, Paraná, Brazil.

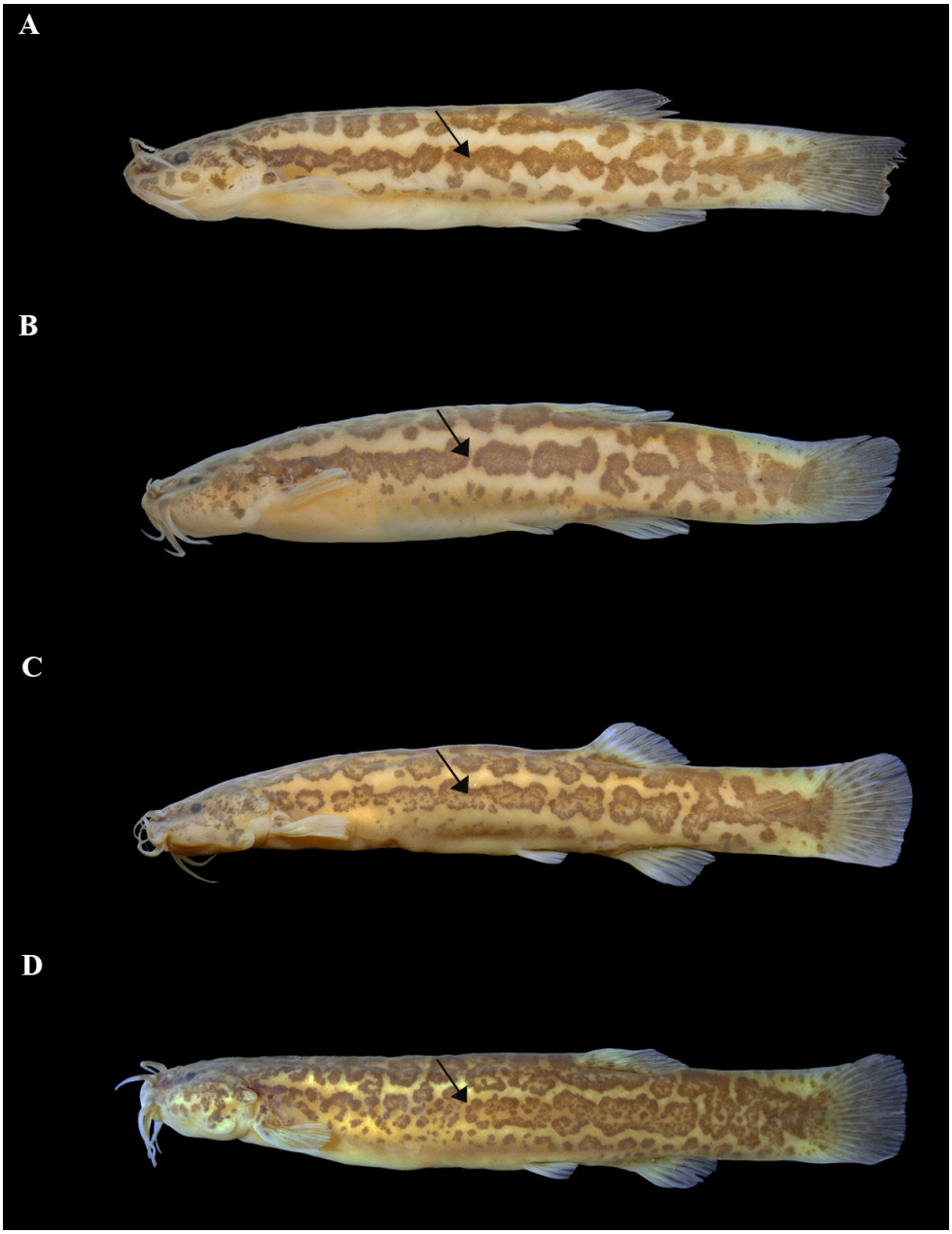

FIGURE 2 | Ontogenetic variation in the color pattern within *Cambeva marginimaculata*, NUP 14591, paratypes. **A.** 25.7 mm SL; **B.** 26.3 mm SL; **C.** 38.9 mm SL; **D.** 45.3 mm SL. Arrows indicate rounded brown blotches of varying size and irregular shape, with dark brown edges that are sometimes connected.

remaining congeners by having 34–37 vertebrae (*vs*. 38 or 39 in *C. gamabelardense*), and 10–12 ribs (*vs*. 14 in *C. panthera* and 14 or 15 in *C. gamabelardense*). Additionally, *C. marginimaculata* differs from *C. panthera* by having the tip of the maxillary barbel reaching between the posterior region of the eye and the opercular odontode plate (*vs*. tip of the maxillary barbel reaching the middle of the pectoral-fin base), and the distal portion of the pelvic fin reaching the anterior portion or first third of the dorsal fin in a vertical line (*vs*. distal portion of the pelvic fin reaching the middle portion of the

dorsal fin in a vertical line). In addition, *C. marginimaculata* differs from sister species indicated by the COI gene tree, *C. davisi*, and *C. perobana* by having the first pectoral-fin ray forming a short to moderately long filament, measuring between 20–30% of the length of the longest pectoral-fin ray (*vs.* absence of filament on the first pectoral-fin ray); and from *C. marliae* sp. n. by having 32–36 premaxillary teeth (*vs.* 44–46), and an entirely ossified epiphyseal bar (*vs.* inconspicuous and incomplete epiphyseal bar).

Description. Morphometric data presented in Tab. 1. Body elongated, trunk cylindrical near head, and gradually becoming laterally compressed towards caudal fin. In lateral view, dorsal profile of body straight, slightly convex from the anterior region to the insertion of dorsal fin. Ventral surface of the body slightly convex from tip of the snout to the insertion of the pelvic fin. Caudal peduncle smoothly continuous with trunk profile; ventral profile slightly concave from pelvic fin to end of peduncle.

TABLE 1 | Morphometric data of *Cambeva marginimaculata* (N = 20, including holotype). Values of range (minimum-maximum), mean, and standard deviation (SD).

	Holotype	Range	Mean	SD
Standard length (mm)	33.0	33.0–80.5	49.5	–
Percent of standard length				
Trunk	41.5	40.3–46.0	42.1	1.5
Preanal length	69.1	60.4–74.5	69.8	2.8
Prepelvic length	58.2	53.5–61.4	56.6	2.0
Pelvic-anal fins distance	10.0	10.0–14.2	12.9	1.0
Caudal-peduncle length	20.0	15.9–22.1	19.4	1.3
Scapular-girdle width	15.8	15.4–17.5	16.3	0.5
Pectoral-fin length	18.2	11.5–20.8	15.3	2.2
Pelvic-fin length	9.1	8.5–11.0	9.7	0.7
Anal-fin length	16.4	15.0–17.3	16.4	0.7
Predorsal length	64.2	61.3–67.0	64.5	1.6
Body length	82.7	82.0–87.1	84.5	1.5
Dorsal-fin length	21.8	17.5–21.8	19.5	1.5
Body depth	13.6	12.9–19.1	15.2	2.1
Dorsal-fin base length	11.2	10.0–13.5	12.0	0.9
Anal-fin base length	8.8	8.0–10.3	9.0	0.6
Caudal-peduncle depth	13.0	11.1–14.7	12.6	0.8
Head length	7.6	17.1–21.8	18.9	1.1
Percent of head length				
Head width	80.4	78.4–96.1	86.8	4.4
Nasal-barbel length	51.1	44.9–77.9	55.5	8.0
Maxillary-barbel length	51.1	50.0–77.9	60.3	6.8
Rictal-barbel length	50.0	47.5–79.2	60.1	8.5
Snout length	35.9	35.8–48.3	40.1	3.3
Interorbital	21.7	17.3–28.8	23.3	2.8
Mouth width	34.8	27.3–39.0	33.1	2.9
Eye diameter	10.9	7.5–14.5	10.1	1.7
Supraorbital pores s6 distance	13.0	12.2–17.7	14.7	1.5

Head depressed, trapezoidal in dorsal view. Eyes visible in lateral view, elliptical, covered by thin and translucent skin, located dorsolaterally on anterior region of head, aligned longitudinally with the nasal barbel. Anterior nostril larger than posterior, surrounded by a fleshy flap of skin continuous with the base of the nasal barbel. Posterior nostril partially surrounded by a thin flap of skin. Gill openings not constricted, forming a free fold reaching base of pectoral fin.

Mouth subterminal, with posteriorly directed margins in ventral view. Lower lip with conspicuous fleshy lobes along lateral edges, continuous with base of rictal barbels. Lips bearing small, rounded papillae of approximately equal size. Barbels with broad bases, gradually tapering toward tips. Nasal barbel originating from posterolateral region of anterior nostril, its free tip extending beyond infraorbital pores i10 when adpressed against the head. Maxillary barbel originating from corner of mouth, its tip reaching anterior region of interopercular plate of odontodes when adpressed to head. Rictal barbel originating from corner of mouth, slightly shorter than maxillary barbel. Pectoral fin with straight distal margin, I,6* rays (20); first unbranched ray prolonged as a short filament. Pelvic fin with rounded distal margin, not reaching urogenital papilla, with I,4* rays (20); origin anterior to that of dorsal fin; inner margins very close to each other. Dorsal fin with rounded distal margin, II,7* rays (16) or II,6 rays (4); origin at vertical through end of pelvic-fin base. Anal fin elongate, with convex distal margin and slightly shorter than dorsal fin, with II,5* rays (19) or II,6 rays (1); origin at vertical through last third of dorsal-fin base. Caudal fin with truncated distal margin; upper caudal-fin plate with I+5* rays (20) and lower plate with I+4 rays (1) or I+6* rays (19).

Osteology. Mesethmoid with straight to slightly concave anterior margin and short cornua with tapered distal tips (Fig. 3A). Anterior cranial fontanel restricted to small rounded opening located immediately anterior to epiphyseal bar. Posterior cranial fontanel long and wide, extending from posterior portion of frontals to parieto-supraoccipital. Epiphyseal bar entirely ossified, longer than wide. Antorbital expanded anteriorly and elongated posteriorly, extending over anterior third of autopalatine. Barbular bone elongated, with medial process on anterior margin. Sphenotic, prootic, and pterosphenoid completely fused. Vomer arrow-shaped with long posterior process extending to parasphenoid. Parasphenoid with long and pointed posterior process, reaching basioccipital. Weberian capsule with small lateral openings and anterior margin fused to basioccipital.

Premaxilla rectangular with 32(3) or 36(2) conical teeth of similar size, arranged in three irregular rows. Dentary with 33(1) or 35(1) spatulate teeth extending from base of coronoid process to near dentary symphysis (Fig. 4A), in one to four rows. Maxilla boomerang-shaped, shorter than premaxilla. Autopalatine with concave lateral margin; slightly convex anterior margin; slightly concave medial margin and long posterior process extending over posterior portion of metapterygoid. Metapterygoid large and laminar, connected to quadrate by cartilage.

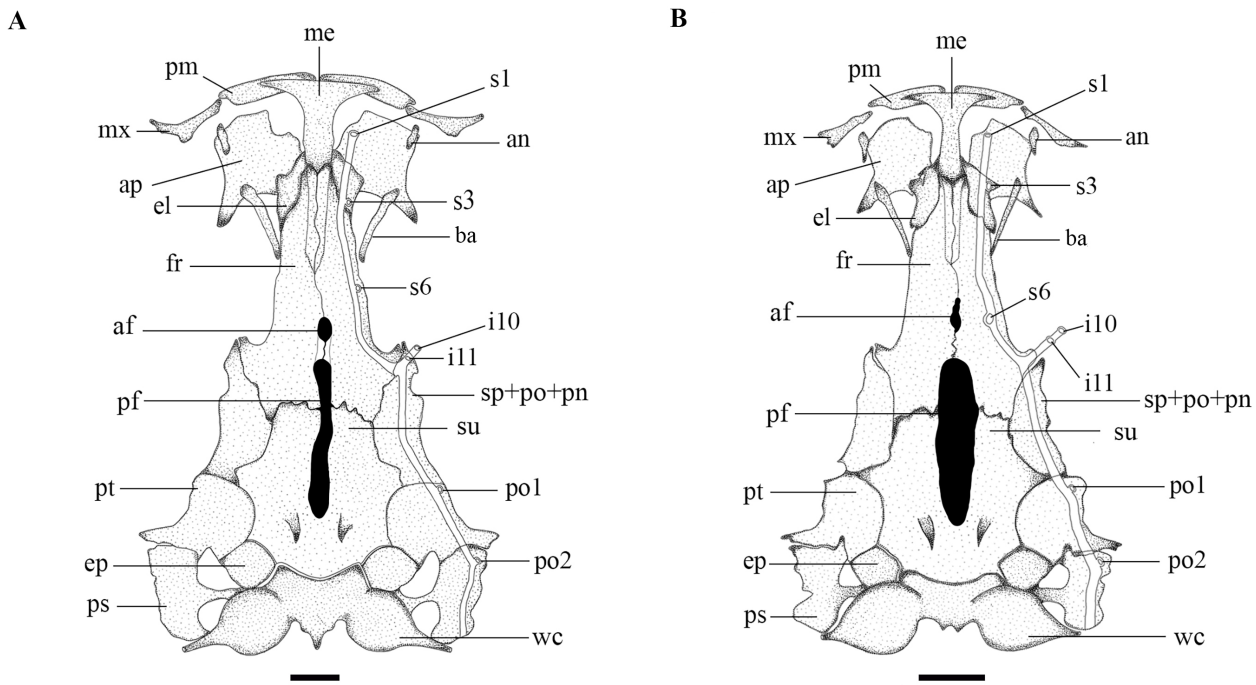

FIGURE 3 | Dorsal view of neurocranium of **A.** *Cambeva marginimaculata*, NUP 25877, paratype, 58.8 mm SL. **B.** *Cambeva marliae*, NUP 25878, paratype, 43.5 mm SL. Abbreviations: af, anterior fontanel; an, antorbital; ap, autopalatine; ba, barbular bone; ep, epioccipital; fr, frontal; le, lateral ethmoid; i10 and i11, infraorbital sensory pores of the laterosensory system; me, mesethmoid; mx, maxilla; pf, posterior fontanel; pm, premaxilla; po1 and po2, postotic sensory pores 1 and 2; ps, posttemporo-supracleithrum; pt, pterotic; s1 s3, and s6, supraorbital sensory pores of the laterosensory system; sp + po + pn, sphenotic–prootic-pterosphenoid complex bone; su, parieto-supraoccipital; wc, Weberian capsule. Scale bars = 1 mm.

Quadrate L-shaped with deep concavity on anterior portion. Hyomandibula well developed; dorsal margin with concavity (Fig. 5A). Opercle longer than interopercle. Opercular odontophores ovoid to rounded with 11(1) or 10(4) conical odontodes, gradually increasing in size posteriorly, arranged in five irregular transverse rows. Interopercular plate elongated, with 23(2) or 24(3) conical odontodes concentrated posteriorly, arranged in two transverse rows.

Ventral hypohyal trapezoid-shaped. Anterior ceratohyal elongated and broader at extremities. Posterior ceratohyal short and triangular. Eight (4) or nine (1) branchiostegal rays: rays 1 to 5 in contact with anterior ceratohyal (5), two rays in contact with interceratohyal cartilage (5), and one (4) or two (1) rays in contact with posterior ceratohyal. Posterior branchiostegal rays broader distally (Fig. 6A). Urohyal with anterior portion expanded, two elongated lateral protuberances with broad bases, tapering distally. Posterior region elongated and narrow, shorter than lateral processes.

Basibranchials 2 and 3 elongated, connected by cartilage; basibranchial 2 slightly larger than basibranchial 3. Basibranchial 4 hexagonal in shape and entirely cartilaginous. Hypobranchial 1 elongated with cartilaginous tips, slightly larger than basibranchial 2. Hypobranchial 2 larger than hypobranchial 3, with large cartilaginous area in distal region. Five elongated ceratobranchials with cartilaginous anterior tips. Ceratobranchial 3 with concavity on posterior margin. Ceratobranchial 5 with

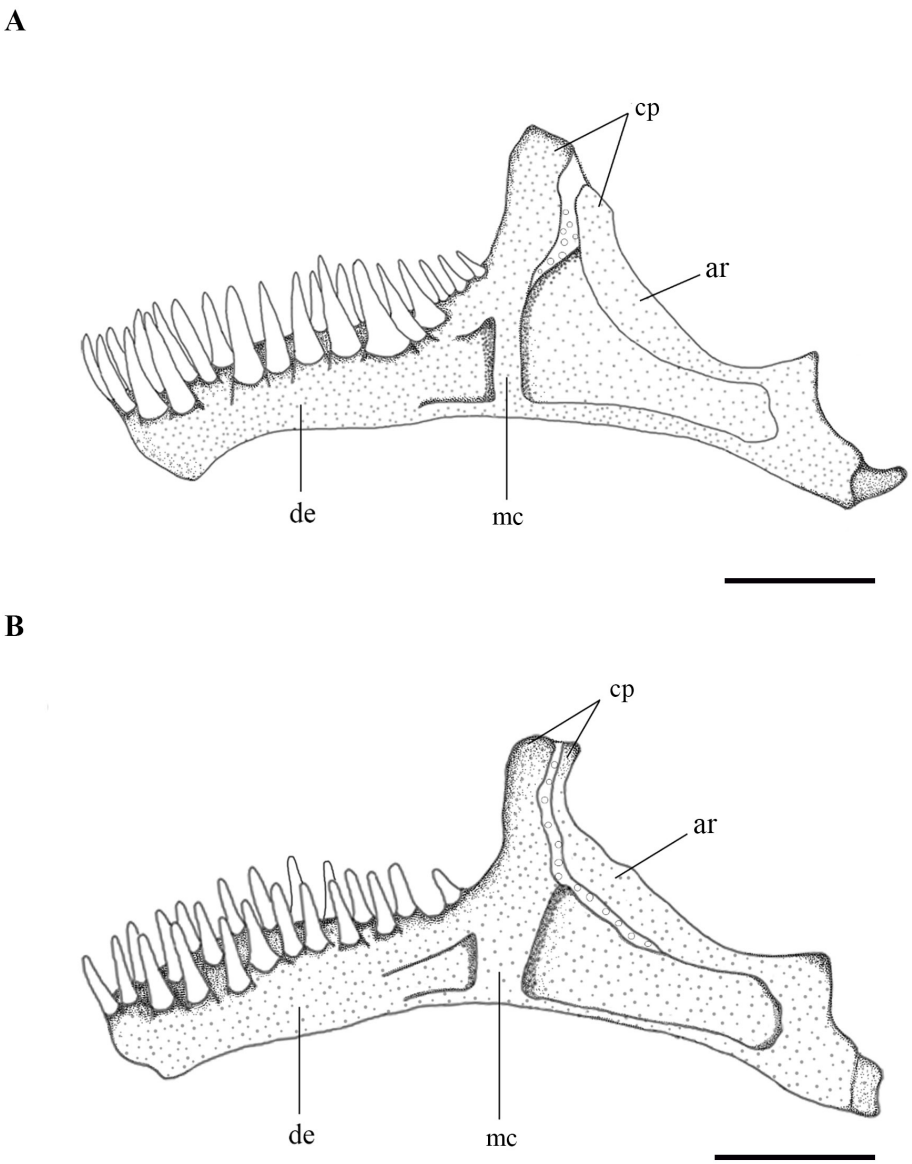

FIGURE 4 | Medial view of lower jaw of **A**. *Cambeva marginimaculata*, NUP 25877, paratype, 58.8 mm SL. **B.** *Cambeva marliae*, NUP 25878, paratype, 43.5 mm SL. Abbreviations: ar, anguloarticular; cp, coronoid process; de, dentary; mc, Meckel's cartilage. Scale bars = 1 mm.

16(1), 19(2), or 22(1) conical, elongated, and pointed teeth arranged in three irregular rows. Four epibranchials: epibranchial 1 with concavity at anterior end, L-shaped; epibranchial 2 more elongated than epibranchials 1, 3, and 4; epibranchial 3 slightly shorter; epibranchial 4 rectangular. Pharyngobranchial 3 straight and elongated, shorter than basibranchial 3. Pharyngobranchial 4 ossified and connected to upper pharyngeal tooth plate with 13(1), 14(2), or 18(2) elongated, conical, and pointed teeth arranged in up to three irregular rows; teeth increasing in size posteriorly (Fig. 7A).

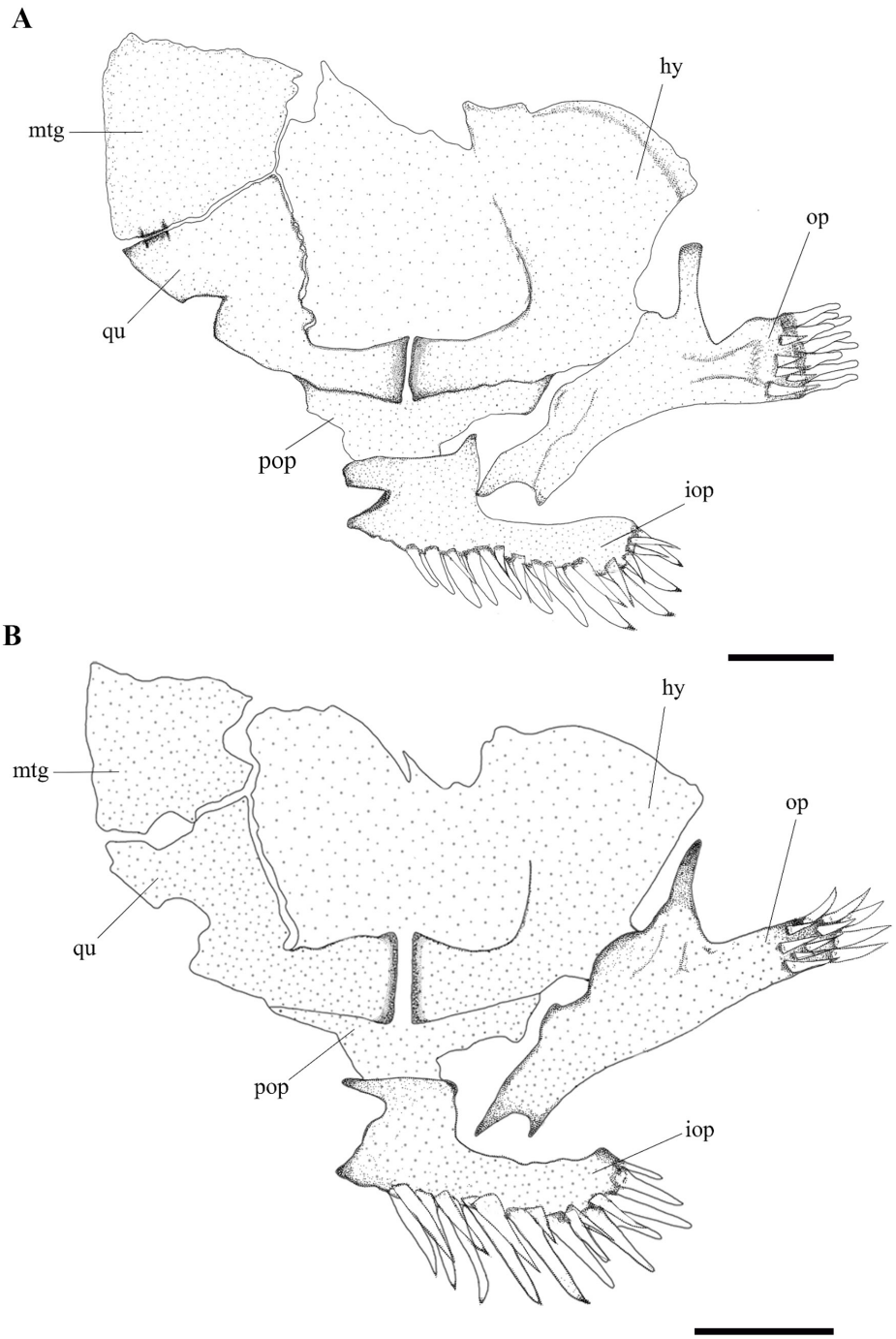

FIGURE 5 | Lateral view of left suspensory of **A.** *Cambeva marginimaculata*, NUP 25877, paratype, 58.8 mm SL. **B.** *Cambeva marliae*, NUP 25878, paratype, 43.5 mm SL. Abbreviations: hy, hyomandibula; iop, interopercle; mtg, metapterygoid; op, opercle; pop, preopercle; qu, quadrate. Scale bars = 1 mm.

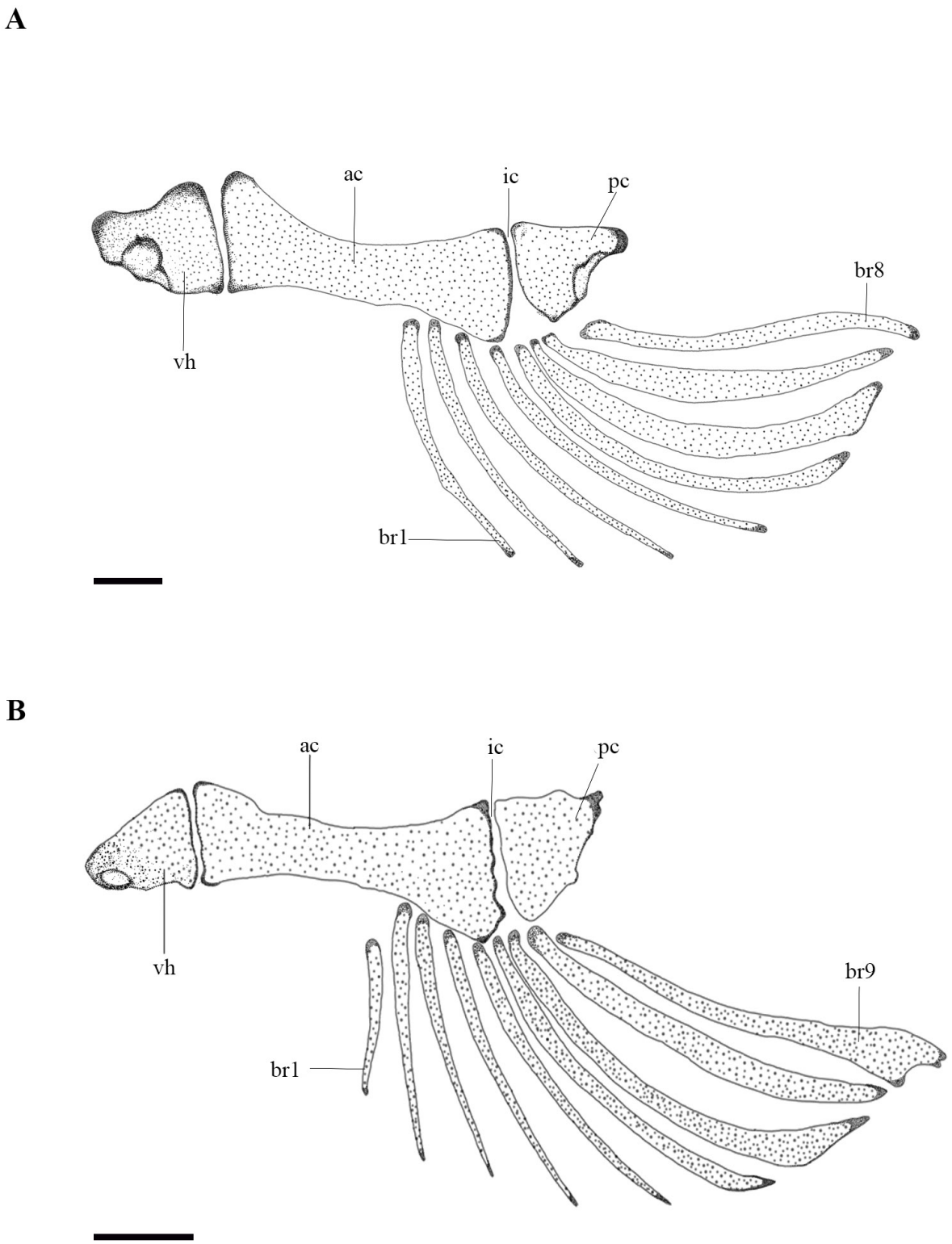

FIGURE 6 | Ventral view of left hyoid arch of **A.** *Cambeva marginimaculata*, NUP 25877, paratype, 58.8 mm SL. **B.** *Cambeva marliae*, NUP 25878, paratype, 43.5 mm SL. Abbreviations: ac, anterior ceratohyal; br1–8, branchiostegal rays 1 to 8; br1–9, branchiostegal rays 1 to 9 for B; ic, interceratohyal; pc, posterior ceratohyal; vh, ventral hypohyal. Scale bars = 1 mm.

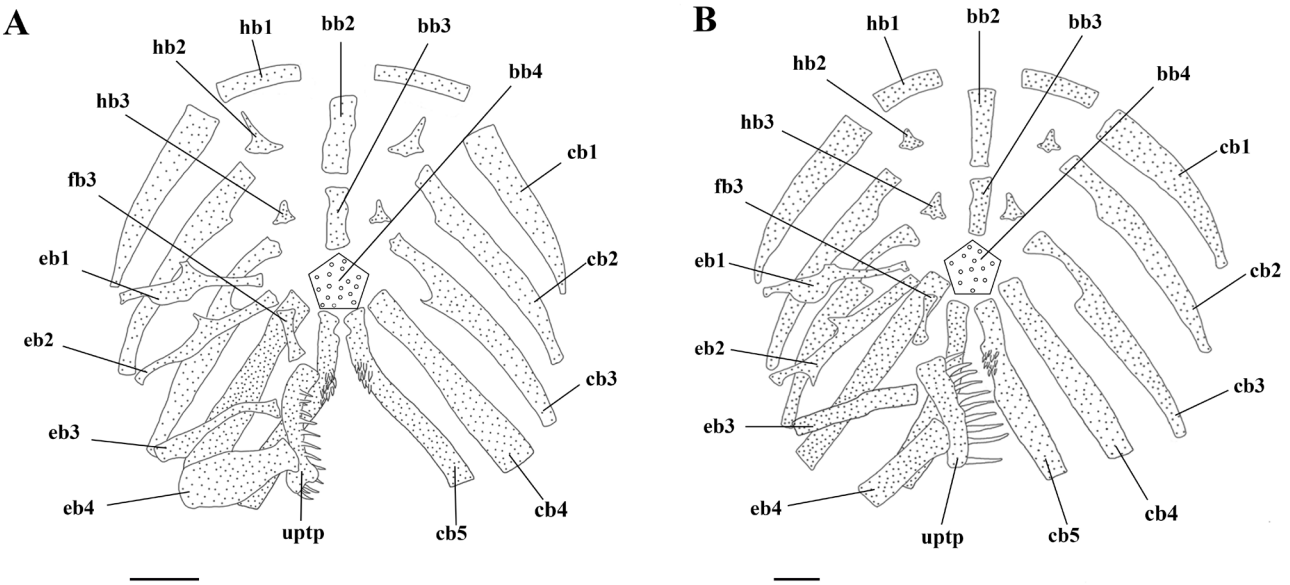

FIGURE 7 | Dorsal view of gill arches (right dorsal elements not show) of **A.** *Cambeva marginimaculata*, NUP 25877, paratype, 58.8 mm SL. **B.** *Cambeva marliae*, NUP 25878, paratype, 43.5 mm SL. Abbreviations: bb2–4, basibranchials 2 to 4; cb1–5, ceratobranchials 1 to 5; eb1–5, epibranchials 1 to 5; hb1–3, hypobranchials 1 to 3; pb3, pharyngobranchial 3; uptp, upper pharyngeal tooth plate. Scale bars = 1 mm.

Dorsal fin with eight pterygiophores (5), first located anterior to neural spine of 17th (2), 18th (1), or 19th (2) post-Weberian vertebrae. Anal fin with six pterygiophores (5), first located anterior to hemal spine of 20th (3) or 21st (2) post-Weberian vertebrae. Procurrent caudal-fin rays 17(1), 18(1), or 19(3) dorsally, and 12(1), 13(2), or 14(2) ventrally. Upper caudal plate with one unbranched ray and five branched rays; hypurals 4 and 5 fused to each other, and hypural 3 either free or fused with others. Single lower caudal plate with one unbranched ray and six branched rays (Fig. 8A). Parhypural and hypurals 1 and 2 co-ossified and fused, forming caudal centrum. Post-Weberian vertebrae 34(1), 35(2), 36(1), or 37(1); ribs 11(4) or 13(1).

Laterosensory system. Laterosensory canals with simple (non-dendritic) branches ending in single pores. Supraorbital sensory canal complete, containing three pores: pore s1 between anterior nares, pore s3 between posterior nares, and pore s6 in interorbital region. Infraorbital sensory canal incomplete, with pore i10 at outer lateral margin of eye, and pore i11 lateral to posterior margin of eye. Postotic pore po1 lateral to anterior margin of opercular odontode plate. Pore po2 lateral to midpoint of opercular plate. Lateral line canal with two pores above base of the pectoral fin and posterior to gill opening.

Coloration in alcohol. Head, flank, and dorsum light yellow, with rounded brown blotches edged with dark brown; blotches on flank irregularly arranged and of variable size, with some larger than opercular odontode plate. Ventral region of head and body yellowish and without blotches. Barbels dark brown. Fins light yellow, with small blotches scattered across caudal and dorsal fins; anal and pectoral fins with small brown blotches on basal region, and pelvic fins without blotch.

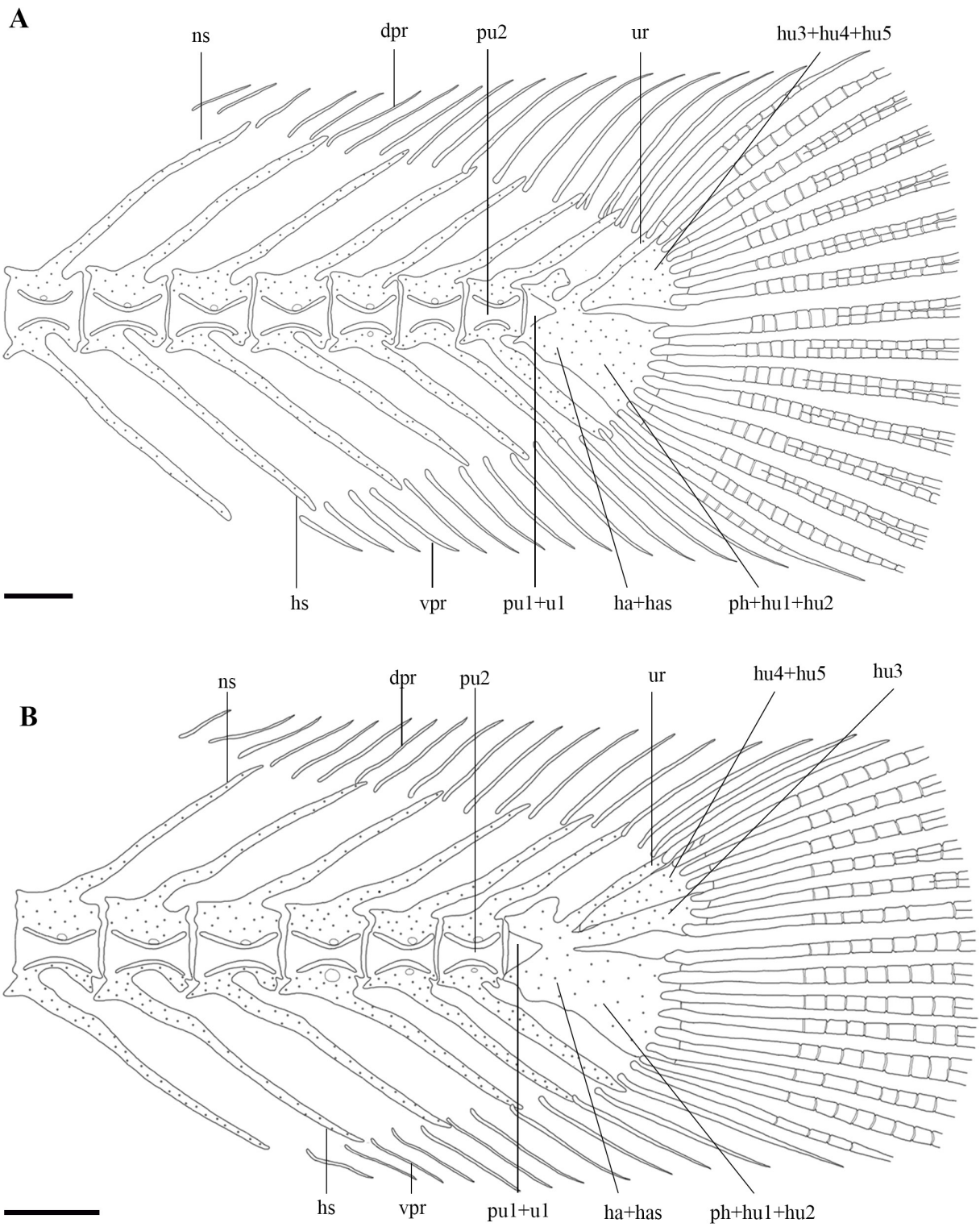

FIGURE 8 | Left lateral view of the caudal peduncle of **A.** *Cambeva marginimaculata*, NUP 25877, paratype, 58.8 mm SL. **B.** *Cambeva marliae*, NUP 25878, paratype, 43.5 mm SL. dpr, dorsal procurrent caudal-fin rays; ha + has, complex hypurapophysis composed of hypurapophysis and secondary hypurapophysis; hs, hemal spine; hu3, hypural 3; hu4 + hu5, complex plate formed by co-ossification of hypurals 4 and 5; ns, neural spine; ph + hu1 + hu2, complex plate formed by co-ossification of hypurals 1 and 2 and parhypural; pu1 + u1, complex centrum composed of pleural centrum 1 and ural centrum 1; pu2, pleural centrum; ur, uroneural; vpr, ventral procurrent caudal-fin rays. Scale bars = 1 mm.

Geographical distribution. *Cambeva marginimaculata* is known from the rio Piquiri basin (upper Paraná) and the lower rio Paraná basin, in the state of Paraná, Brazil. See further details on the geographic distribution of *C. marliae*.

Ecological notes. The type-locality of *C. marginimaculata* is located at an elevation of 450 m above sea level (Fig. 9). The surrounding area is characterized by an urban environment, and the stream crosses an area of modified landscape, indicating a high degree of anthropization. Near the site, an area of pasture and water channeling was observed. *C. marginimaculata* was collected with *Hypostomus ancistroides* (Ihering, 1911), *Rhamdia quelen* (Quoy & Gaimard, 1824), and *Psalidodon bifasciatus* (Garavello & Sampaio, 2010).

Conservation status. *Cambeva marginimaculata* has an estimated EOO of 4963.865 km² (< 5,000 km² under criterion B1) and an AOO of 60,000 km² (< 500 km² under criterion B2). Although these values have a geographically restricted distribution, the available data are insufficient to infer a continuing decline, severe fragmentation, or



FIGURE 9 | Type-locality of *Cambeva marginimaculata*, unnamed stream, tributary of rio Melissa, rio Piquiri basin, upper rio Paraná basin, Paraná State, Brazil.

extreme fluctuations as required under subcriteria (a–c) of criterion B. In 2024, some of these locations were sampled, but *C. marginimaculata* was not found among the collected individuals. It was noted that many of these water bodies were silted, which may have contributed to the absence of the species. However, these observations do not allow a robust assessment of population trends or a documented continuing decline in habitat quality across its entire distribution. Based on the presently available evidence and following the International Union for Conservation of Nature (IUCN) Categories and Criteria (IUCN Standards and Petitions Subcommittee, 2024) it is recommended that *C. marginimaculata* be classified as Least Concern (LC), although further monitoring is recommended given its restricted distribution and habitat alteration.

Etymology. The specific name of *C. marginimaculata* highlights the main diagnostic feature of the species that distinguishes it from most congeners. The specific name *marginimaculata* (*marginis* = "margin" + *maculata* = "blotch") refers to the presence of blotches with a visible outline or border on the body of the species. An adjective.

Cambeva marliae, new species

urn:lsid:zoobank.org:act:700A8A35-1C22-421B-BDBC-31A868F9FB4A

(Figs. 3B–8B, 10–11; Tab. 2)

Trichomycterus sp. 1 —Gubiani *et al*., 2010:3 (Fish, Toledo urban streams, São Francisco Verdadeiro, River drainage, upper Paraná River basin, state of Paraná, Brazil; *partim*: NUP 8520).

Trichomycterus sp. 2 —Gubiani *et al*., 2010:3 (Fish, Toledo urban streams, São Francisco Verdadeiro, River drainage, upper Paraná River basin, state of Paraná, Brazil; *partim*: NUP 8524).

Trichomycterus sp. 3 —Gubiani *et al*., 2010:3 (Fish, Toledo urban streams, São Francisco Verdadeiro, River drainage, upper Paraná River basin, state of Paraná, Brazil; *partim*: NUP 8521).

Holotype. NUP 26968, 70.8 mm SL, municipality of Toledo, rio Jacutinga, tributary of rio Marreco, rio São Francisco Verdadeiro, lower rio Paraná, 24°41'58"S 53°46'11"W, 9 Oct 2007, Gerpel.

Paratype. All from Brazil, Paraná State. Upper rio Paraná basin: rio Piquiri basin: NUP 25734, 3, 52.2–58.9 mm SL, municipality of São Pedro do Iguaçu, unnamed stream, 24°56'37.9"S 53°53'36.8"W, 25 Oct 2024, I. C. Martins, A. Frota & V. A. Teixeira. Lower rio Paraná basin: rio São Francisco Verdadeiro: MHNCI 13135, 1, 68.0 mm SL, municipality of Toledo, rio Panambi, tributary of rio Marreco, 24°41'55"S 53°45'25"W, 27 Feb 2009, Gerpel. MZUEL 24222, 1, 60.0 mm SL, municipality of Toledo, rio Jacutinga, tributary of rio Marreco, 24°41'58"S 53°46'11"W, 7 Oct 2008, Gerpel. NUP 8506, 2, 31.0–55.0 mm SL, same data as holotype. NUP 8520, 2, 26.0–50.0 mm SL, municipality of Toledo, rio Jacutinga, tributary of rio Marreco, 24°43'15"S 53°46'22"W, 9 Aug 2009, Gerpel. NUP 8523, 1, 40.0 mm SL, municipality of Toledo, rio Jacutinga, tributary of rio Marreco, 24°42'56"S 53°46'21"W, 9 Aug 2009, Gerpel. NUP 8525, 1, 33.0 mm SL, municipality of Toledo, rio Jacutinga, tributary of rio Marreco, 24°43'15"S 53°46'22"W, 9 Aug 2009, Gerpel. NUP 8533, 1, 41.6 mm SL, municipality of Toledo, rio Jacutinga, tributary of rio Marreco, rio São Francisco



FIGURE 10 | *Cambeva marliae*, NUP 26968, holotype, 70.8 mm SL, rio Jacutinga, tributary of rio Marreco, rio São Francisco Verdadeiro, lower rio Paraná, municipality of Toledo, Paraná, Brazil. Scale bar = 10 mm.

Verdadeiro, lower rio Paraná, 24°42'56"S 53°46'21"W, 9 Jun 2008, Gerpel. NUP 25737, 3, 48.8–49.9 mm SL, municipality of Toledo, unnamed stream, 24°42'56"S 53°46'21"W, 24 Oct 2024, I. C. Martins, A. Frota & V. A. Teixeira. NUP 25878, 2 c&s, 52.0–56.0 mm SL, municipality of Toledo, rio Panambi, tributary of rio Marreco, 24°41'55"S 53°45'25"W, 9 Oct 2009, Gerpel. NUP 25903, 7, 27.0–65.0 mm SL, municipality of Toledo, rio Jacutinga, tributary of rio Marreco, 24°43'14"S 53°46'19"W, 1 Dec 2007, Gerpel. UFRGS 30245, 1, 66.0 mm SL, municipality of Toledo, rio Jacutinga, tributary of rio Marreco, 24°42'56"S 53°46'21"W, 9 Aug 2009, Gerpel. Rio São Francisco Falso: NUP 25834, 1, 52.5 mm SL, municipality of São Pedro do Iguaçu, unnamed stream, tributary of rio São Francisco Falso, 24°56'36"S 53°53'37"W, 11 Feb 2023, H. Brandão, L. E. P. Kampfert, D. R. Blanco, J. C. Maicrovicz & E. Ribeiro.

Non-types. Brazil, Paraná State, municipality of Toledo, rio Jacutinga, tributary of rio Marreco: CIG 1542, 2, 53.0–63.0 mm SL, CIG 1553, 4, 55.0–73.0 mm SL, 24°42'09"S 53°46'39.8"W, 1 Dec 2007, Gerpel. CIG 1564, 1, 58.0 mm SL, 24°43'14.5"S 53°46'19"W, 8 Oct 2007, Gerpel.

Diagnosis. *Cambeva marliae* differs from all congeners except *C. botuvera* Costa, Feltrin & Katz, 2021, *C. cubataonis* (Bizerril, 1994), and *C. urubici* Costa, Feltrin & Katz, 2021 by the presence of rounded coalescent blotches about the size of the opercular odontophore, forming along the midlateral region of the body a discontinuous stripe in the anterior region of the body and the caudal peduncle (*vs*. absence of a midlateral stripe on the body; or when present, a continuous longitudinal stripe as in *C. naipi* (Wosiacki & Garavello, 2004), *C. pascuali* (Ochoa, Silva, Costa e Silva, Oliveira & Datovo, 2017), *C. perkos* (Datovo, Carvalho & Ferrer, 2012), *C. piraquara* dos Reis, Wosiacki, Ferrer, Donin & da Graça, 2023, some specimens of *C. perobana*, and small individuals of *C. poikilos* (Ferrer & Malabarba, 2013); and a broad stripe, the size of two or three opercular odontophores in some individuals of *C. zonata* (Eigenmann, 1918)). *C. marliae* differs from *C. botuvera*, and *C. urubici* by having 36 vertebrae (*vs*. 39 or 40 vertebrae in *C. urubici* and *C. botuvera*); from *C. cubataonis* by having 12 opercular odontodes (*vs*. 7–10), and 17.1–24.7% in the interorbital distance (*vs*. 25.7–33.3% in the interorbital distance); and additionally, from *C. urubici* by having 12 or 13 ribs (*vs*. 15 or 16 ribs). Additionally, *C. marliae* can be distinguished from *C. botuvera*, *C. cubataonis*, and *C. urubici* by some larger specimens (45.0 mm SL) having a small extension forming a small filament (Fig. 11) on the first pectoral-fin ray (*vs*. absence). *C. marliae* is further distinguished from the syntopic species *C. marginimaculata* by having 44–46 premaxillary teeth (*vs*. 32–36), and an inconspicuous and incomplete epiphyseal bar (*vs*. entirely ossified epiphyseal bar).

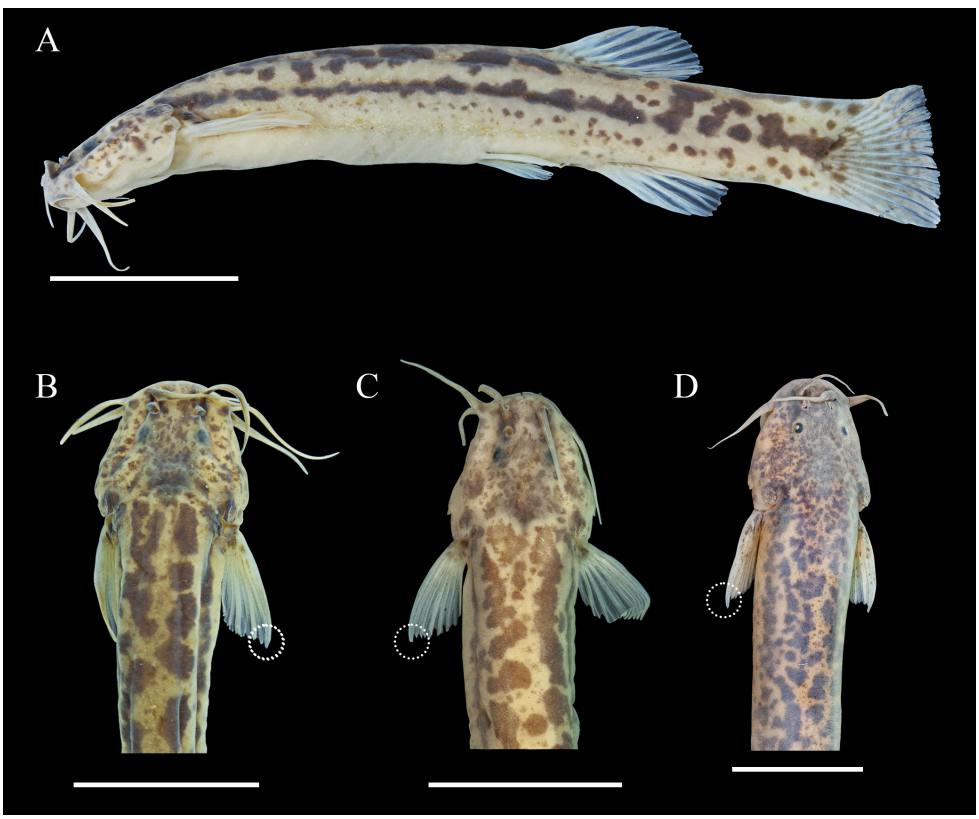

FIGURE 11 | Color variation and filamentous extension of the first unbranched pectoral-fin ray in *Cambeva marliae*. **A.** Lateral view, NUP 8533, 41.6 mm SL; **B.** NUP 8533, 41.6 mm SL; **C.** NUP 8523, 40.0 mm SL; **D.** NUP 25834, 52.5 mm SL. Dashed circle indicates filament. Scale bars = 10 mm.

Description. Morphometric data presented in Tab. 2. Body elongate, trunk approximately cylindrical near head, gradually becoming laterally compressed towards caudal fin. Dorsal profile of trunk slightly convex from anterior half of body to origin of dorsal fin. Ventral surface of body slightly convex. Dorsal and ventral profiles of caudal peduncle concave.

Head depressed, trapezoidal in dorsal view, broader posteriorly. Snout rounded in dorsal view. Eyes visible in lateral view, elliptical, covered by thin and translucent skin, located dorsolaterally on anterior region of head; orbital margin not free. Anterior and posterior nostrils rounded, equal in size or smaller than eye diameter; surrounded by skin continuous with base of nasal barbel. Posterior nostril bordered anterolaterally by a thin layer of skin. Gill openings not constricted, joined to isthmus anteriorly and forming a free fold.

Mouth subterminal, with posteriorly directed margins in ventral view. Lower lip with fleshy lobes along lateral edges, internal to base of rictal barbels. Lips with small papillae. Larger papillae on inner surface of upper lip. Barbels with broad bases, gradually tapering toward tips. Nasal barbel extending slightly beyond pore i11, originating from posterolateral region of anterior nostril skin. Maxillary barbel reaching anterior region of interopercular odontode plate. Rictal barbel slightly shorter than maxillary barbel.

TABLE 2 | Morphometric data of *Cambeva marliae* (N = 20, including holotype). Values of range (minimum-maximum), mean, and standard deviation (SD).

	Holotype	Range	Mean	SD
Standard length (mm)	70.8	31.5–69.0	46.3	–
Percent of standard length				
Trunk	29.0	39.4–47.0	43.5	2.4
Preanal length	49.9	67.9–77.5	72.6	2.1
Prepelvic length	40.1	52.7–61.5	57.1	2.2
Pelvic-anal fins distance	9.7	9.8–16.4	13.3	1.6
Caudal-peduncle length	12.3	17.1–22.9	19.1	1.3
Scapular-girdle width	10.5	14.0–18.7	15.8	1.1
Pectoral-fin length	9.1	11.4–18.4	15.2	1.8
Pelvic-fin length	6.7	8.3–11.1	9.5	0.7
Anal-fin length	11.7	12.0–21.0	16.0	1.9
Predorsal length	44.2	63.7–70.2	66.6	2.0
Body length	55.4	77.1–91.4	84.7	3.1
Dorsal-fin length	13.2	15.2–22.1	18.5	1.9
Body depth	9.4	12.6–18.8	15.0	1.6
Dorsal-fin base length	8.1	7.3–13.1	10.7	1.4
Anal-fin base length	5.1	4.7–9.6	7.8	1.1
Caudal-peduncle depth	8.7	11.1–13.7	12.0	0.7
Head length	13.6	16.4–21.3	18.6	1.3
Percent of head length				
Head width	10.2	75.0–98.9	87.1	6.2
Nasal-barbel length	7.7	38.8–72.4	56.2	9.9
Maxillary-barbel length	7.3	41.4–78.3	60.3	10
Rictal-barbel length	7.1	48.9–90.8	63.4	11
Snout length	5.7	29.9–43.7	38.5	3.7
Interorbital	3.2	17.1–24.7	21.1	2.0
Mouth width	5.4	32.5–41.4	36.9	3.0
Eye diameter	1.0	7.4–12.9	10.6	1.3
Supraorbital pores s6 distance	6.8	9.6–19.3	14.8	2.3

Pectoral fin with straight distal margin, I,6* rays (20); first unbranched ray prolonged as filament. Pelvic fin with rounded distal margin, not reaching anterior margin of urogenital papilla, with I,4* rays (20); origin anterior to that of dorsal fin; inner margins very close to each other. Dorsal fin with rounded distal margin, II,7* rays (18) and II,6 rays (2); origin at vertical through end of pelvic-fin base. Anal fin elongate with convex distal margin, slightly shorter than dorsal fin, with II,5* rays (18), II,6 rays (1), or II,3 rays (1); origin at vertical through last third of dorsal-fin base. Caudal fin with truncated distal margin; upper caudal-fin plate with I+5* rays (20) and lower plate with I+6* rays (19) or I+5 rays (1).

Osteology. Mesethmoid with straight to slightly concave anterior margin and short horn with tapered distal ends (Fig. 3B). Anterior cranial fontanel restricted to small opening located between frontals and epiphyseal bar. Posterior cranial fontanel long and wide, extending from posterior portion of frontals to parieto-supraoccipital. Epiphyseal bar inconspicuous and incomplete. Antorbital expanded anteriorly and elongated posteriorly, extending over anterior third of autopalatine. Barbular bone elongated, thin, and straight. Sphenotic, prootic, and pterosphenoid completely fused. Vomer arrow-shaped with long posterior process extending to parasphenoid. Posterior process of parasphenoid long, extending to anterior portion of basioccipital. Weberian capsule with small lateral openings and anterior margin fused to basioccipital.

Premaxilla rectangular, narrowed at medial portion, with 44(1) or 46(1) conical teeth of similar size distributed in three irregular rows. Dentary with 37(1) or 39(1) spatulate teeth extending from base of coronoid process to near dentary symphysis (Fig. 4B) in one to four rows. Maxilla boomerang-shaped, slightly shorter than premaxilla. Autopalatine with concave lateral margin; medial margin slightly concave and posterior process long, extending over posterior portion of metapterygoid. Metapterygoid large and laminar, connected to quadrate by cartilage.

Quadrate L-shaped with concavity on anterior portion. Hyomandibula well developed; dorsal margin with concavity (Fig. 5B). Opercular plate rounded. Opercular odontophores ovoid to rounded with 12(2) conical odontodes, gradually curving medially and increasing in size posteriorly, arranged in four irregular transverse rows. Interopercular plate elongated, in contact with ventral margin of hyomandibula, with 25(1) or 27(1) conical odontodes concentrated posteriorly, arranged in two transverse rows.

Ventral hypohyal trapezoid-shaped. Anterior ceratohyal elongated and wider at extremities. Posterior ceratohyal short and triangular. Nine branchiostegal rays articulated with hyoid arch (2): rays 1 to 6 in contact with anterior ceratohyal, one ray in contact with interceratohyal cartilage, and two rays in contact with posterior ceratohyal. Posterior branchiostegal rays broader distally (Fig. 6B). Urohyal with anterior portion expanded, bearing two elongated lateral projections with broad bases, tapering distally. Posterior region elongated and narrow, shorter than lateral processes.

Basibranchials 2 and 3 elongated, connected by cartilage; basibranchial 2 slightly larger than basibranchial 3. Basibranchial 4 hexagonal in shape and entirely cartilaginous. Hypobranchial 1 elongated, with cartilaginous tips, similar in size to basibranchial 2. Hypobranchial 2 similar in size to hypobranchial 3, with large cartilaginous area on distal region. Five elongated ceratobranchials with cartilaginous anterior extremities. Ceratobranchial 3 with concavity on posterior margin. Ceratobranchial 5 bearing 17(1)

or 18(1) elongated, conical, and pointed teeth arranged in three irregular rows. Four epibranchials: epibranchial 1 with concavity at anterior end, L-shaped; epibranchial 2 more elongated than epibranchials 1, 3, and 4; epibranchial 3 slightly shorter; epibranchial 4 rectangular. Pharyngobranchial 3 straight and elongated, similar in size to basibranchial 3. Pharyngobranchial 4 ossified and connected to upper pharyngeal tooth plate, bearing 20(1) or 24(1) elongated, conical, and pointed teeth arranged in up to three irregular rows; teeth increasing in size posteriorly (Fig. 7B).

Dorsal fin with eight pterygiophores (2), first anterior to neural spine of the 17th or 19th post-Weberian vertebrae. Anal fin with six or seven pterygiophores, first anterior to hemal spine of the 20th (1) or 21st (1) post-Weberian vertebrae. Procurrent caudal-fin rays 22(2) dorsally and 14(1) or 15(1) ventrally. Upper caudal-fin plate with one unbranched ray and five branched rays; hypural 3 free, and hypurals 4 and 5 fused. Lower caudal-fin plate single, with one unbranched ray and six branched rays (Fig. 8B). Parhypural and hypurals 1 and 2 co-ossified and fused to compound caudal centrum. Post-Weberian vertebrae 36(2); ribs 12(1) or 13(1).

Laterosensory system. Laterosensory canals with simple (non-dendritic) tubes ending in single pores. Supraorbital sensory canal continuous and connected posteriorly to infraorbital sensory canals. Supraorbital sensory canal containing pores s1, s3, and s6. Two pores in infraorbital sensory canal: pore i10, at outer lateral margin of the eye, and pore i11, lateral to posterior margin of eye. Postotic pore po1 lateral to anterior portion of opercular odontode plate. Pore po2 lateral to midpoint of opercular plate. Two pores in lateral line above base of pectoral fin and posterior to gill openings.

Coloration in alcohol. Head, flank, and dorsum light yellow, with discontinuous dark brown blotches forming longitudinal stripe along midlateral line of body, from posterior region of opercular plate to caudal peduncle. Diameter of blotches variable, gradually becoming smaller toward ventral region. Blotches denser and more rounded on dorsal region, extending to base of caudal fin. Ventral region of head and body yellowish and without blotches. Barbels light yellow or light brown. Fins light yellow, with small blotches scattered throughout caudal fin; dorsal, anal, and pectoral fins with small brown blotches on basal region, and pelvic fins without blotches.

Ecological notes. The type-locality of *C. marliae* is at 543 m above sea level (Fig. 12). The site is in a rural area surrounded by pastures, with a narrow strip of forest partially protecting its banks. *Cambeva marliae* was collected with *Characidium* aff. *zebra* Eigenmann, 1909, *Gymnotus* aff. *carapo* Linnaeus, 1758, *G. paraguensis* Albert & Crampton, 2003, *G. pantanal* Fernandes, Albert, Daniel-Silva, Lopes, Crampton & Almeida-Toledo, 2005, *Hoplias* sp., *Hypostomus ancistroides* (Ihering, 1911), *Phalloceros harpagos* Lucinda, 2008, *Poecilia reticulata* Peters, 1859, *Psalidodon bifasciatus* (Garavello & Sampaio, 2010), *P. fasciatus* (Cuvier, 1819), *Saxatilia britskii* (Kullander, 1982), and *Serrapinnus calliurus* (Boulenger, 1900).



FIGURE 12 | Type-locality of *Cambeva marliae*, rio Jacutinga, tributary of rio Marreco, rio Piquiri basin, upper rio Paraná basin, Paraná State, Brazil.

Conservation status. *Cambeva marliae* has an estimated EOO of 584,126 km² (< 5,000 km² in criterion B1) and an AOO of 20,000 km² (< 500 km² in criterion B2). The species is known only from a few scattered localities, and its presence in other environments remains uncertain, which limits the real understanding of its distribution. The type-locality and surrounding areas are characterized by rural landscapes with pasturelands and partial riparian vegetation, suggesting potential diffuse threats such as habitat degradation, siltation, and water quality alteration associated with agricultural activities. Additionally, the occurrence of non-native species in the area may represent an additional ecological pressure. However, there is currently insufficient information regarding population size, trends, and the magnitude or continuity of these potential threats. Given these uncertainties, it is not possible to reliably assess whether the species meets the criteria for a threatened category. Therefore, following the International Union for Conservation of Nature (IUCN) Categories and Criteria (IUCN Standards

and Petitions Subcommittee, 2024), it is recommended that *Cambeva marliae* be classified as Data Deficient (DD), pending further ecological and distributional studies.

Molecular data. A total of 163 COI gene sequences (510 bp) were used, including one sequence of *C. marginimaculata* and five of *C. marliae*. The final alignment comprised 91 unique haplotypes (Tab. **S1**). The genetic distances (K2P) between species groups showed that *C. marginimaculata* is 2.0% divergent from *C. marliae*, and both species are more than 2.0% divergent from the remaining species included in the analysis. The complete results of genetic distances between all sequences and species groups are provided in the supplementary material (Tabs. **S2**, **S3**). The Bayesian tree (Fig. 13A) and the maximum likelihood (Fig. **S4**) indicated that *C. marginimaculata* and *C. marliae* form sister lineages to each other and to *C. perobana*.

The molecular delimiters indicated overall congruence in recognizing *C. marginimaculata* and *C. marliae* as distinct species (Fig. 13B). The ASAP, PTP, and mGMYC methods support the hypothesis that both represent evolutionarily independent lineages. However, the sGMYC method suggested that the two morphotypes and *C. perobana* represent the same species. The full results of the species delimiters sGMYC and mGMYC are provided as supplementary material, respectively (Figs. **S5**, **S6**).

Geographical distribution. *Cambeva marginimaculata* and *C. marliae* are known from the rio Piquiri basin (upper Paraná) and the lower rio Paraná basin, in the state of Paraná, Brazil (Fig. 14). *Cambeva marginimaculata* has a relatively wide distribution within these basins. In the rio Piquiri basin, it occurs in an unnamed stream (type locality), a tributary of the rio Melissa, as well as in the rio Santa Fé, rio Pioneiro, rio São Camilo, riacho Quati, rio Piquirizinho, rio das Antas, córrego Taquari and rio do Bagre. In the lower rio Paraná basin basin, the species has been recorded in the rio São Francisco Verdadeiro (including the rio do Cedro, rio Pinheirinho, and córrego São Francisco) and in the rio Guaçu (ribeirão Lageado). *Cambeva marliae*, in turn, has a more restricted distribution. In the rio Piquiri basin, the species is known only from an unnamed stream. In the lower rio Paraná basin, it was found in the rio São Francisco Falso (in an unnamed stream) and in the rio São Francisco Verdadeiro (including the rio Jacutinga – type locality, rio Panambi, and an unnamed stream). Although both species occur in the same basins, they have not been recorded at the same sampling sites.

Etymology. *Cambeva marliae* is named in honour of Marli Cristina Campos, a technician in the Nupélia-UEM ichthyological collection. Marli has worked at Nupélia for 33 years and has extensive experience with biological material. In addition, she took part in several fish collection activities. A noun in a genitive case.

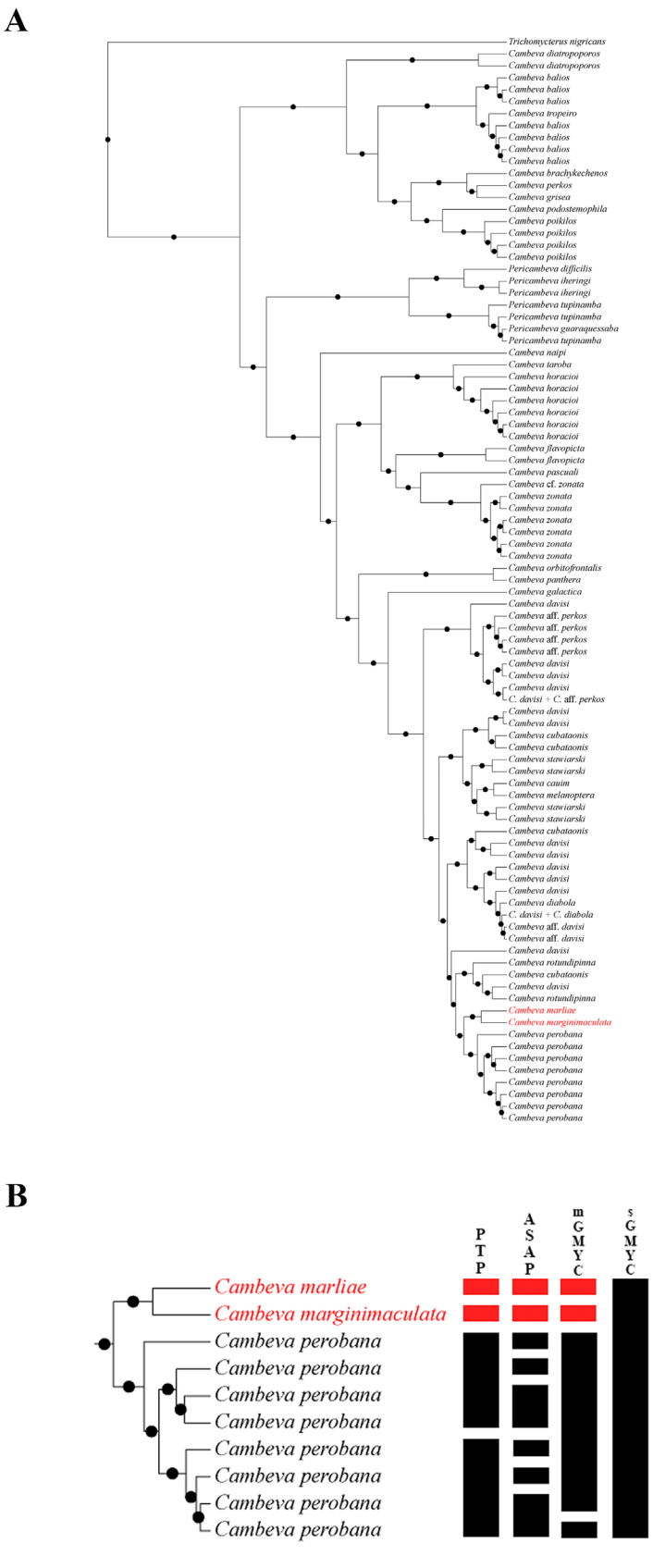

FIGURE 13 | **A.** Bayesian gene tree constructed from *Cambeva* COI sequences. **B.** Bayesian COI gene tree with species delimitation results. Vertical bars represent species delimitation from Assemble Species by Automatic Partition (ASAP), Poisson Tree Process (PTP) and Generalized Mixed Yule Coalescent (GMYC). Circles represent posterior probability ≥ 0.90. *Cambeva marginimaculata* and *C. marliae* are shown in red.

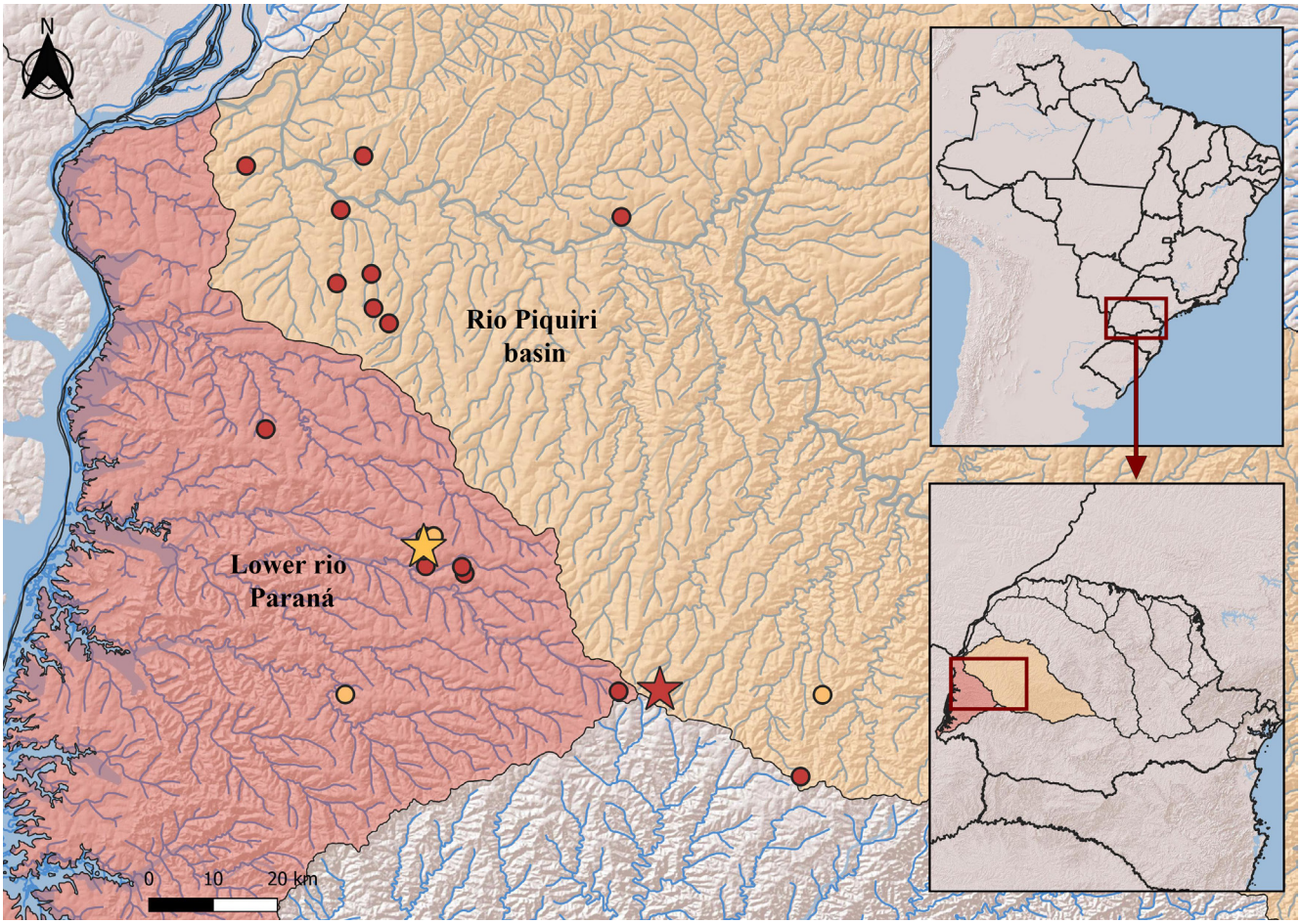

FIGURE 14 | Partial map of South America, highlighting Brazil and the state of Paraná, showing the geographic distribution of *Cambeva marginimaculata* and *C. marliae* in the rio Piquiri and lower rio Paraná basins. Red and yellow symbols represent *C. marginimaculata* and *C. marliae*, respectively. Stars represent their type localities.

DISCUSSION

Cambeva marginimaculata and *C. marliae* are distinguished from their closest congeners by a combination of morphological characters. *Cambeva marginimaculata* is characterized by brown blotches with dark brown margins scattered over the body, a pigmentation pattern absent in *C. perobana* and *C.* aff. *davisi*. *Cambeva marliae* bears coalescent blotches forming a distinct, discontinuous midlateral band. Although *C. perobana* and some specimens of *C.* aff. *davisi* may also exhibit a midlateral band (Haseman, 1911; Nascimento *et al.*, 2017; Martins *et al.*, 2024), the band in *C. perobana* is narrow (Martins *et al.*, 2024), whereas in *C. marliae* it is conspicuous. Moreover, both *C. perobana* and *C.* aff. *davisi* lacks the short filament formed by the first pectoral-fin ray present in *C. marliae*. Opercular odontode counts also differ, with *C. marliae* possessing 10–11 (*vs.* 39–40 in *C.* aff. *davisi* (dos Reis *et al.*, 2020b)).

Molecular data further corroborate the distinction of both species. *Cambeva marginimaculata* shows a genetic distance of 2% from *C. marliae*, 2.8% from *C. perobana*, and 3.9% from *C.* aff. *davisi*. Meanwhile, *C. marliae* has a genetic distance of 2% from *C.*

perobana and 3.6% from *C.* aff. *davisi*. Although values of 2% or higher are commonly used as indicators of interspecific differentiation in fishes based on DNA barcoding (Hebert *et al*., 2003; Hubert, Renno, 2006; Hanner *et al*., 2011), this threshold does not represent a biological rule. Therefore, following Queiroz (2007), species delimitation should be grounded on evidence rather than on isolated criteria.

The discordance among delimitators shown in Fig. 12B may be related to the sensitivity of sGMYC, as this method tends to be more conservative in species delimitation, particularly in cases of recent divergence, heterogeneous speciation rates, or low sample sizes per species (Talavera *et al*., 2013; Luo *et al*., 2018). These factors may lead the BEAST substitution model to fail in accurately detecting the transition point between intra- and interspecific processes (Fujisawa, Barraclough, 2013). Therefore, such incongruence does not invalidate the results but rather reinforces the importance of considering other biological evidence for species identification (Pereira *et al*., 2013; Camelier *et al*., 2018; Luo *et al*., 2018; Serrano *et al*., 2019; Donin *et al*., 2022). In this context, mGMYC showed greater congruence with the morphological data, recognizing the two taxa as distinct, probably due to its greater flexibility compared to sGMYC and its ability to account for multiple transition points (Fujisawa, Barraclough, 2013).

The ML and Bayesian analyses recovered broadly congruent topologies (Fig. 12A), with two main clades within the obtained *Cambeva* sequences. *Cambeva marginimaculata* and *C. marliae* were recovered as sister group (PP = 0.94; BS = 70%), with multiple individuals of *C. marliae* forming a strongly supported monophyletic clade (PP = 0.99; BS = 100%), while *C. marginimaculata* was represented by a single haplotype. Both new species were recovered as sister group to *C. perobana*, though this relationship received low support in both analyses (PP = 0.57; BS = 18%), which may partly reflect the limitations of single-locus mitochondrial analyses in resolving recently diverged lineages. The phylogenetic relationship between these species may reflect recent diversification driven by geographic isolation among the Piquiri, Ivaí, and Lower Paraná river basins. Geological events and climatic shifts over time played a key role in drainage reorganization and the formation of the current hydrographic basins, increasing the complexity of river systems. These factors contributed to the speciation and genetic structuring observed in freshwater fish assemblages (Hubert, Renno, 2006; Ribeiro, 2006; Morais-Silva *et al*., 2018; Cassemiro *et al*., 2023; dos Reis *et al*., 2025a).

Cambeva marginimaculata and *C. marliae* can be assigned to the *Cambeva* clade β (Beta) proposed by Costa *et al*. (2023), a regionally structured clade comprising species from the upper rio Paraná basin and adjacent coastal drainages. Clade β is not diagnosable by morphological characters; however, molecular analyses using COI, CytB, and RAG markers provide strong support for its monophyly and suggest a geographically structured diversification pattern (Costa *et al*., 2023). Multi-locus incorporating nuclear markers would be desirable to further clarify the phylogenetic relationships within this group and to strengthen the assignment of the new species to clade β.

Some Trichomycterinae species were recently studied using a comparative osteological approach by Costa (2026), who restricted *Cambeva* to the clades previously designated as β (Beta) and γ (Gama) by Costa *et al.* (2023). In this paper, Costa (2026) erected two new genera to accommodate species formerly assigned to the clade α (Alpha) in *Cambeva*: *Pericambeva*, for species of the *C. iheringi* (= *Pericambeva iheringi*)

group, and *Pseudocambeva*, for species of the *C. variegata* (= *Pseudo. variegata*) group. The placement of *C. marginimaculata* and *C. marliae* within clade β, as demonstrated by the molecular analyses of the present study, is fully consistent with the revised generic concept of Costa (2026), confirming their assignment to *Cambeva*.

Until now, two valid species of *Cambeva* had been recorded from the rio Piquiri basin: *C.* aff. *davisi* and *C. perobana* (dos Reis *et al*., 2020a; Martins *et al*., 2024). *Cambeva marginimaculata* and *C. marliae* represent two additional records of the genus in this basin, increasing the number of species known from the area. In the lower rio Paraná ecoregion, Pereira *et al.* (2021) reported the occurrence of *C.* aff. *davisi*, grouping specimens into four morphotypes, some of which share the same geographic area. The identification of *C. davisi* in this ecoregion should be undertaken with caution due to the high morphological variation. Although the specimens examined by Pereira *et al*. (2021) were not directly examined in the present study, a comparison based on the morphological descriptions and figures provided by those authors suggests that some of these morphotypes may share diagnostic traits with *C. marginimaculata* and *C. marliae*, particularly given the geographic proximity of the collection localities. Nevertheless, a definitive assignment of those morphotypes to the species described herein requires their direct examination, which we recommend as a priority for future taxonomic work on *Cambeva* in the rio Paraná basin.

The two new species exhibit distinct distribution patterns, with *C. marginimaculata* occurring across a broader area and *C. marliae* restricted to a narrower range, based on the available data. Nevertheless, both species occur in tributaries of the upper and lower rio Paraná. The upper rio Paraná basin is characterized by heterogeneous altitudinal gradients (Dagosta *et al*., 2024) and comprises several sub-ecoregions in the state of Paraná (Abell *et al*., 2008), including the rio Piquiri sub-ecoregion (dos Reis *et al*., 2020a). The Piquiri basin is a branched drainage network with multiple rapids, waterfalls, and narrow stretches (Cavalli *et al*., 2018) and may have been affected by headwater capture events. Such events promote connections among basins, thereby driving diversification and faunal mixing (Hubert, Renno, 2006). Similar processes have been documented in *Psalidodon bifasciatus* (Neves *et al*., 2020; dos Reis *et al*., 2020a) and may also account for headwater captures between streams of the lower Paraná and Piquiri tributaries, showing a distributional pattern similar to that observed in the new species. Thus, the biogeographic contexts of each sub-ecoregion within the rio Paraná basin in the state of Paraná may be directly related to the distribution patterns observed, contributing to the understanding of assemblage structure in these areas.

The description of *C. marginimaculata* and *C. marliae* further emphasizes the importance of headwater streams, which act as regulators of water quality and serve as habitats for small-sized species (Freeman *et al*., 2007; Meyer *et al*., 2007). Small streams are under constant threat from human activities (Meyer *et al*., 2007) and are more likely to be overlooked by legal protection policies (Wohl, 2017). Therefore, the identification of new species highlights the need for conservation strategies targeting these environments, not only to preserve local biodiversity but also to ensure the ecological integrity of connected freshwater systems.

Comparative material examined. Brazil. *Cambeva cubataonis*: rio Cubatão basin: NUP 19196, 1, 33.0 mm SL. *Cambeva davisi*: rio Iguaçu basin: NUP 4008, 11, 22.1–82.1 mm SL. NUP 15914, 67, 21.3–78.2 mm SL. NUP 16097, 29, 28.9–79.8 mm SL. NUP 17364, 34, 38.7–74.3 mm SL. *Cambeva horacioi*: rio Ivaí basin: MCP 54181, 88.1 mm SL. *Cambeva perobana*: rio Ivaí basin: NUP 11727, 1, 52.0 mm SL. NUP 14307, 4, 33.0–53.0 mm SL. NUP 6069, 3, 50.5–51.3 mm SL. Rio Piquiri basin: NUP 23907, 75.9 mm SL. *Cambeva pascuali*: NUP 23343, 3, 34.9–48.3 mm SL.

ACKNOWLEDGMENTS

To Augusto Frota, Wladimir Domingues, Valdenir de Souza, and Valmir Teixeira for their assistance with the fieldwork. To Programa de Pós-Graduação em Ecologia de Ambientes Aquáticos Continentais (PEA) and Instituto de Pesquisas em Limnologia, Ictiologia e Aquicultura (Nupélia) for the logistic support.

REFERENCES

- **Abell R, Thieme ML, Revenga C, Bryer M, Kottelat M, Bogutskaya N *et al*.** Freshwater ecoregions of the world: a new map of biogeographic units for freshwater biodiversity conservation. BioScience. 2008; 58(5):403–14. https://doi.org/10.1641/B580507
- **Agostinho AA, Pelicice FM, Petry AC, Gomes LC, Júlio HF.** Fish diversity in the upper Paraná River basin: habitats, fisheries, management and conservation. Aquat Ecos Health Manag. 2007; 10(2):174–86. https://doi.org/10.1080/14634980701341719
- **Agostinho AA, Vazzoler AMAM, Thomaz SM.** The high Paraná River basin: limnological and ichthyological aspects. In: Tundisi JG, Bicudo CEM, Matsumura-Tundisi T, editors. Limnology in Brazil. Rio de Janeiro: ABC/SBL; 1995. p.59–103.
- **Arratia FG, Chang GA, Marque SM, Rojas MG.** About *Bullockia* gen. nov., *Trichomycterus mendozensis* n. sp. and revision of the family Trichomycteridae (Pisces, Siluriformes). Stud Neotrop Fauna Environ. 1978; 13(3–4):157–94. https://doi.org/10.1080/01650527809360539
- **Bockmann FA, Casatti L, de Pinna MCC.** A new species of trichomycterid catfish from the rio Paranapanema basin, southeastern Brazil (Teleostei: Siluriformes), with comments on the phylogeny of the family. Ichthyol Explor Freshw. 2004; 15(3):225–42.
- **Bonetto AA.** The Paraná River system. In: Davies BR, Walkers KF, editors. The ecology river systems. Dordrecht: Dr. W. Junk Publishers; 1986. p.541–55.
- **Britski HA, Langeani F.** *Pimelodus paranaensis*, sp. n., um novo Pimelodidae (Pisces, Siluriformes) do Alto Paraná, Brasil. Rev Bras Zool. 1988; 5(3):409–17. https://doi.org/10.1590/S0101-81751988000300006
- **Camelier P, Menezes NA, Costa-Silva GJ, Oliveira C.** Molecular and morphological data of the freshwater fish *Glandulocauda melanopleura* (Characiformes: Characidae) provide evidences of river captures and local differentiation in the Brazilian Atlantic Forest. PLoS ONE. 2018; 13(3):e0194247. https://doi.org/10.1371/journal.pone.0194247
- **Cassemiro FAS, Albert JS, Antonelli A, Menegotto A, Wüest RO, Cerezer F *et al*.** Landscape dynamics and diversification of the megadiverse South American freshwater fish fauna. PNAS. 2023; 120(2):e2211974120. https://doi.org/10.1073/pnas.2211974120

- **Cavalli D, Frota A, Lira AD, Gubiani ÉA, Margarido VP, Graça WJ.** Update on the ichthyofauna of the rio Piquiri basin, Paraná, Brazil: a conservation priority area. Biota Neotrop. 2018; 18(2):e20170350. https://doi.org/10.1590/1676-0611-bn-2017-0350
- **Costa WJEM.** Description de huit nouvelles espèces du genre *Trichomycterus* (Siluriformes: Trichomycteridae), du Brésil oriental. RFAH. 1992; 18(4):101–10.
- **Costa WJEM.** Comparative morphology and generic classification of catfishes of the *Trichomycterus* lineage (Siluriformes: Trichomycteridae). Taxonomy. 2026; 6:20. https://doi.org/10.3390/taxonomy6010020
- **Costa WJEM, Feltrin CRM, Mattos JLO, Dalcin RH, Abilhoa V, Katz AM.** Morpho-molecular discordance? Re-approaching systematics of *Cambeva* (Siluriformes: Trichomycteridae) from the Guaratuba-Babitonga-Itapocu area, Southern Brazil. Fishes. 2023; 8(2):63. https://doi.org/10.3390/fishes8020063
- **Costa WJEM, Feltrin CRM, Mattos JLO, Katz AM.** Top mountain areas of subtropical southern Brazil sheltering four new small-ranged catfishes (Siluriformes, Trichomycteridae): relationships and taxonomy. Evol Syst. 2024; 8(2):199–218. https://doi.org/10.3897/evolsyst.8.126393
- **Dagosta FCP, Monção MS, Nagamatsu BA, Pavanelli CS, Carvalho FR, Lima FCT *et al*.** Fishes of the upper rio Paraná basin: diversity, biogeography and conservation. Neotrop Ichthyol. 2024; 22(1):e230066. https://doi.org/10.1590/1982-0224-2023-0066
- **Donin LM, Ferrer J, Carvalho TP.** Taxonomical study of *Trichomycterus* (Siluriformes: Trichomycteridae) from the Ribeira de Iguape River basin reveals a new species recorded in the early 20th century. J Fish Biol. 2020; 96(4):886–904. https://doi.org/10.1111/jfb.14278
- **Donin LM, Ferrer J, Carvalho F.** Uncertainties and risks in delimiting species of *Cambeva* (Siluriformes: Trichomycteridae) with single-locus methods and geographically restricted data. Neotrop Ichthyol. 2022; 20(3):e220019. https://doi.org/10.1590/1982-0224-2022-0019
- **Drummond AJ, Suchard MA, Xie D, Rambaut A.** Bayesian phylogenetics with BEAUti and the BEAST 1.7. Mol Biol Evol. 2012; 29(8):1969–73. https://doi.org/10.1093/molbev/mss075
- **Ferrer J, Malabarba LR.** Taxonomic review of the genus *Trichomycterus* Valenciennes (Siluriformes: Trichomycteridae) from the laguna dos Patos system, Southern Brazil. Neotrop Ichthyol. 2013; 11(2):217–46. https://doi.org/10.1590/S1679-62252013000200001
- **Freeman MC, Pringle CM, Jackson CR.** Hydrologic connectivity and the contribution of stream headwaters to ecological integrity at regional scales. J Am Water Resour Assoc. 2007; 43(1):5–14. https://doi.org/10.1111/j.1752-1688.2007.00002.x
- **Fricke R, Eschmeyer WN, Fong JD.** Eschmeyer's catalog of fishes: genera/species by family/subfamily [Internet]. San Francisco: California Academy of Science; 2026a. Available from: http://researcharchive.calacademy.org/research/ichthyology/catalog/SpeciesByFamily.asp
- **Fricke R, Eschmeyer WN, Van der Laan R.** Eschmeyer's catalog of fishes: genera, species, references. [Internet]. San Francisco: California Academy of Science; 2026b. Available from: http://researcharchive.calacademy.org/research/ichthyology/catalog/fishcatmain.asp
- **Fujisawa T, Barraclough TG.** Delimiting species using single-locus data and the generalized mixed yule coalescent approach: a revised method and evaluation on simulated data sets. Syst Biol. 2013; 62(5):707–24.
- **Gubiani EA, Daga VS, Frana VA, Graça WJ.** Fish, Toledo urban streams, São Francisco Verdadeiro River drainage, upper Paraná River basin, state of Paraná, Brazil. Check List. 2010; 6(1):45–48. https://doi.org/10.15560/6.1.045
- **Hall TA.** BioEdit: a user-friendly biological sequence alignment editor and analysis program for Windows 95/98/NT. Nucleic Acids Symp Ser. 1999; 41:95–98.
- **Hanner R, Floyd R, Bernard A, Collette BB, Shivji M.** DNA barcoding of billfishes. Mitochondrial DNA. 2011; 22(S1):27–36. https://doi.org/10.3109/19401736.2011.596833

- **Haseman JD.** Some new species of fishes from the rio Iguassú. Ann Carnegie Mus. 1911; 7(3–4):374–87.
- **Hebert PDN, Ratnasingham S, De Waard JR.** Barcoding animal life: cytochrome c oxidase subunit 1 divergences among closely related species. Proc R Soc Lond B. 2003; 270(S1):96–399. https://doi.org/10.1098/rsbl.2003.0025
- **Hubert N, Renno J.** Historical biogeography of South American freshwater fishes. J Biogeogr. 2006; 33(8):1414–36. https://doi.org/10.1111/j.1365-2699.2006.01518.x
- **Ivanova NV, Zemlak TS, Hanner RH, Hebert PDN.** Universal primer cocktails for fish DNA barcoding. Mol Ecol Notes. 2007; 7(4):544–48. https://doi.org/10.1111/j.1471-8286.2007.01748.x
- **International Union for Conservation of Nature (IUCN). Standards and petitions committee.** Guidelines for using the IUCN Red List categories and criteria. Version 15.1 [Internet]. Gland; 2024. Available from: http://cmsdocs.s3.amazonaws.com/RedListGuidelines.pdf
- **Katz AM, Barbosa MA, Mattos JLO, Costa WJEM.** Multigene analysis of the catfish genus *Trichomycterus* and description of a new South American trichomycterine genus (Siluriformes, Trichomycteridae). Zoosyst Evol. 2018; 94(2):557–66. https://doi.org/10.3897/zse.94.29872
- **Luo A, Ling C, Ho SYW, Zhu C-D.** Comparison of methods for molecular species delimitation across a range of speciation scenarios. Syst Biol. 2018; 67(5):830–46. https://doi.org/10.1093/sysbio/syy011
- **Maack R.** Geografia física do Estado do Paraná. 2nd ed. Rio de Janeiro: José Olympio; 1981.
- **Martins IC, dos Reis RB, Stabile BHM, Graça WJ.** Iterative taxonomy reveals a new species of *Cambeva* (Siluriformes: Trichomycteridae) with intraspecific variation from the rio Piquiri and Ivaí basin, upper rio Paraná basin, Brazil. Neotrop Ichthyol. 2024; 22(3):e230140. https://doi.org/10.1590/1982-0224-2023-0140
- **Meyer JL, Strayer DL, Wallace JB, Eggert SL, Helfman GS, Leonard NE.** The contribution of headwater streams to biodiversity in river networks. J Am Water Resour Assoc. 2007; 43(1):86–103. https://doi.org/10.1111/j.1752-1688.2007.00008.x
- **Morais-Silva JP, Oliveira AV, Fabrin TM, Diamante NA, Prioli SMAP, Frota A *et al*.** Geomorphology influencing the diversification of fish in small-order rivers of neighboring basins. Zebrafish. 2018; 15(4):389–97. https://doi.org/10.1089/zeb.2017.1551
- **Nascimento RHC, Frantine-Silva W, Souza-Shibatta L, Sofia SH, Ferrer J, Shibatta OA.** Intrapopulational variation in color pattern of *Trichomycterus davisi* (Haseman, 1911) (Siluriformes: Trichomycteridae) corroborated by morphometrics and molecular analysis. Zootaxa. 2017; 4290(3):503–18. https://doi.org/10.11646/zootaxa.4290.3.5
- **Neves MP, Silva PC, Delariva RL, Fialho CB, Netto-Ferreira AL.** First record of *Astyanax bifasciatus* Garavello & Sampaio (Teleostei: Ostariophysi: Characidae) in the rio Piquiri basin, upper Paraná river basin. Check List. 2020; 16(1):93–101. https://doi.org/10.15560/16.1.93
- **Paraná.** Secretaria de Estado do Meio Ambiente e Recursos Hídricos. Bacias hidrográficas do Paraná: série histórica. 2nd ed. Curitiba: SEMA; 2013.
- **Pereira LHG, Castro JRC, Vargas PMH, Gomez JAM, Oliveira C.** The use of an integrative approach to improve accuracy of species identification and detection of new species in studies of stream fish diversity. Genetica. 2021; 149:103–16. https://doi.org/10.1007/s10709-021-00118-6
- **Pereira LHG, Hanner R, Foresti F, Oliveira C.** Can DNA barcoding accurately discriminate megadiverse Neotropical freshwater fish fauna? BMC Genet. 2013; 14(1):1–14. https://doi.org/10.1186/1471-2156-14-20
- **Pereira A, Ribeiro V, Gubiani É, Zacarkim C, Cunico A.** Ichthyofauna of urban streams in the western region of Paraná State, Brazil. Check List. 2014; 10(3):550–55. https://doi.org/10.15560/10.3.550

- **de Pinna MCC, Wosiacki WB.** Family Trichomycteridae (pencil or parasitic catfishes). In: Reis RE, Kullander SO, Ferraris Jr. CJ, editors. Check list of the freshwater fishes of South and Central America. Porto Alegre: Edipucrs; 2003. p.270–90.
- **Pons J, Barraclough TG, Gomes-Zurita J, Cardoso A, Duran DP, Hazell S *et al*.** Sequence Based species delimitation for the DNA taxonomy of undescribed insects. Syst Biol. 2006; 55(4):595–609. https://doi.org/10.1080/10635150600852011
- **Puillandre N, Brouillet S, Achaz G.** ASAP: assemble species by automatic partitioning. Mol Ecol Resour. 2021; 21(2):609–20. https://doi.org/10.1111/1755-0998.13281
- **Queiroz K.** Species concepts and species delimitation. Syst Biol. 2007; 56(6):879–86. https://doi.org/10.1080/10635150701701083
- **Rambaut A.** FigTree-Version 1.4. 4, a graphical viewer of phylogenetic trees. Computer program distributed by the author; 2019. Available from: http://tree.bio.ed.ac.uk/software/figtree
- **Rambaut A, Drummond AJ, Xie D, Baele G, Suchard MA.** Posterior summarization in Bayesian phylogenetics using Tracer 1.7. Syst Biol. 2018; 67(5):901–04. https://doi.org/10.1093/sysbio/syy032
- **dos Reis RB, Frota A, Deprá G C, Ota RR, Graça WJ.** Freshwater fishes from Paraná state, Brazil: an annotated list, with comments on biogeographic patterns, threats, and future perspectives. Zootaxa. 2020a; 4868(4):451–94. https://doi.org/10.11646/zootaxa.4868.4.1
- **dos Reis RB, Frota A, Fabrin TMC, Graça WJ.** A new species of *Cambeva* (Siluriformes, Trichomycteridae) from the rio Ivaí basin, upper rio Paraná basin, Paraná State, Brazil. J Fish Biol. 2020b; 96(2):350–63. https://doi.org/10.1111/jfb.14204
- **dos Reis RB, Martins IC, Stabile BHM, Ferrer J, Oliveira AV, McMahan CD *et al*.** Taxonomy, phylogeny, and conservation of an endangered freshwater fish species from southeastern brazil: revisiting historical descriptions using integrative approaches. Ichthyol Herpetol. 2025b; 113(4):647–66. https://doi.org/10.1643/i2025022
- **dos Reis RB, Stabile BHM, Frota A, Ferrer J, Oliveira AV, Graça WJ.** Recent dispersion routes between freshwater ecoregions evidence headwater captures in southern Brazil: a case study using cryptic species of the Neotropical freshwater fish genus *Cambeva* (Siluriformes: Trichomycteridae). Hydrobiologia. 2025a; 852:873–90. https://doi.org/10.1007/s10750-024-05731-y
- **dos Reis RB, Wosiacki WB, Ferrer J, Donin LM, Graça WJ.** A new species of *Cambeva* (Siluriformes: Trichomycteridae) from an area of high anthropogenic impacts in the headwaters of rio Iguaçu, Southern Brazil. Can J Zool. 2023; 101(6):1–11. https://doi.org/10.1139/cjz-2022-0150
- **Ribeiro AC.** Tectonic history and the biogeography of the freshwater fishes from the coastal drainages of eastern Brasil: an example of faunal evolution associated with a divergent continental margin. Neotrop Ichthyol. 2006; 4(2):225–46. https://doi.org/10.1590/S1679-62252006000200009
- **Rosenthal A, Coutelle O, Craxton M.** Large-scale production of DNA sequencing templates by microtitre format PCR. Nucleic Acids Res. 1993; 21(1):173–74. https://doi.org/10.1093/nar/21.1.173
- **Rozas J, Ferrer-Mata A, Sánchez-DelBarrio JC, Guirao-Rico S, Librado P, Ramos-Onsins SE *et al*.** DnaSP 6: DNA sequence polymorphism analysis of large data sets. Mol Biol Evol. 2017; 34(12):3299–302. https://doi.org/10.1093/molbev/msx248
- **Serrano ÉA, Melo BF, Freitas-Souza D, Oliveira MLM, Utsunomia R, Oliveira C *et al*.** Species delimitation in neotropical fishes of the genus *Characidium* (Teleostei, Characiformes). Zool Scr. 2019; 48(1):69–80. https://doi.org/10.1111/zsc.12318
- **Silva CCF, Matta SLSF, Hilsdorf AWS, Langeani F, Marceniuk AP.** Color pattern variation in *Trichomycterus iheringi* (Eigenmann, 1917) (Siluriformes: Trichomycteridae) from rio Itatinga and rio Claro, São Paulo, Brazil. Neotrop Ichthyol. 2010; 8(1):49–56. https://doi.org/10.1590/S1679-62252010000100007
- **Stevaux C.** The upper Paraná River (Brazil): geomorphology, sedimentology and paleoclimatology. Quat Int. 1994; 21:143–61. https://doi.org/10.1016/1040-6182(94)90028-0

- **Talavera G, Dincã V, Vila R.** Factors affecting species delimitations with the GMYC model: insights from a butterfly survey. Methods Ecol Evol. 2013; 4(12):1101–10. https://doi.org/10.1111/2041-210X.12107
- **Tamura K, Stecher G, Kumar S.** MEGA11: Molecular Evolutionary Genetics Analysis Version 11. Mol BiolEvolution. 2021; 38(7):3022–27. https://doi.org/10.1093/molbev/msab120
- **Taylor WR, Van Dyke G.** Revised procedures for staining and clearing small fishes and other vertebrates for bone and cartilage study. Cybium. 1985; 9(2):107–19.
- **Tchernavin VV.** A revision of some Trichomycterinae based on material preserved in the British Museum (Natural History). Proc Zool Soc London. 1944; 114(1–2):234–75. https://doi.org/10.1111/j.1096-3642.1944.tb00219.x
- **Thompson JD, Higgins DG, Gibson TJ.** CLUSTAL W: improving the sensitivity of progressive multiple sequence alignment through sequence weighting, position-specific gap penalties and weight matrix choice. Nucleic Acids Res. 1994; 22(22):4673–80. https://doi.org/10.1093/nar/22.22.4673
- **Vences M, Miralles A, Brouillet S, Ducasse J, Fedosov A, Kharchev V *et al*.** iTaxoTools 0.1: kickstarting a specimen-based software toolkit for taxonomists. Megataxa. 2021, 6(2):77–92. https://doi.org/10.11646/megataxa.6.2.1
- **Ward RD, Zemlak TS, Innes BH, Last PR, Hebert PDN.** DNA barcoding Australia's fish species. Philos Trans R Soc B. 2005; 360(1462):1847–57. https://doi.org/10.1098/rstb.2005.1716
- **Wohl E.** The significance of small streams. Front Earth Sci. 2017; 11(3):447–456. https://doi.org/10.1007/s11707-017-0647-y
- **Zhang J, Kapli P, Pavlidis P, Stamatakis A.** A general species delimitation method with applications to phylogenetic placements. Bioinformatics. 2013; 29(22):2869–76. https://doi.org/10.1093/bioinformatics/btt499

AUTHORS' CONTRIBUTION

Isadora Carolina Martins: Conceptualization, Data curation, Investigation, Methodology, Visualization, Writing-original draft, Writing-review and editing.

Renan Borges dos Reis: Methodology, Visualization, Writing-review and editing.

Bruno Henrique Mioto Stabile: Methodology, Visualization, Writing-review and editing.

Alessandra Valéria de Oliveira: Conceptualization, Writing-review and editing

Weferson Júnio da Graça: Conceptualization, Funding acquisition, Project administration, Resources, Supervision, Writing-review and editing.

FUNDING INFORMATION

The research was partly funded by the Fundação Araucária (Apoio ao Desenvolvimento Científico e Tecnológico do Paraná) process number: 10558/2016 and 124/2023 for WJG. The Conselho Nacional de Desenvolvimento Científico e Tecnológico (CNPq) granted technical productivity subsidies to WJG (processes 305200/2018–6, 307089/2021–5 and 303571/2024–1). ICM, RBR and BHMS were supported by grants from the Coordenação de Aperfeiçoamento de Pessoal de Nível Superior (CAPES) processes 88887.894166/2023–00, 88887.629034/2021–00, and 88887.629037/2021–00, respectively.

ETHICAL STATEMENT

The collections were authorized by the Ethics Committee on the Use of Animals (CEUA/UEM, authorization Nº 7283090823) and by the SISBIO license (ICMBio), under process 14028–1 of October 12, 2008, issued to WJG.

DATA AVAILABILITY STATEMENT

The authors confirm that the data supporting the conclusions of this study are available in the article and supplementary material.

AI STATEMENT

Some sections of the text were reviewed by two AI tools (Grammarly, ChatGPT) to improve grammatical agreement and correct possible errors. The authors declare that the figures are their own work.

COMPETING INTERESTS

The authors declare no competing interests.

SUPPLEMENTARY MATERIAL

Supplementary Material File

PEER REVIEW REPORT

Reviewers:

Anonymous reviewer #1

Anonymous reviewer #2

The peer review report is available at: Neotropical Ichthyology

HOW TO CITE THIS ARTICLE

- **Martins IC, Reis RB, Stabile BHM, Oliveira AV, Graça WJ.** Morphological and molecular evidence reveals two new species of *Cambeva* (Siluriformes: Trichomycteridae) from the rio Paraná basin, Paraná State, Brazil. Neotrop Ichthyol. 2026; 24(4):e250156. https://doi.org/10.1590/1982-0224-2025-0156

Neotropical Ichthyology

OPEN ACCESS

This is an open access article under the terms of the Creative Commons Attribution License, which permits use, distribution and reproduction in any medium, provided the original work is properly cited.

Distributed under
Creative Commons CC-BY 4.0

© 2026 The Authors.
Published by SBI

Official Journal of the
Sociedade Brasileira de Ictiologia

SBI